République Algérienne Démocratique et Populaire
Ministère de l'Enseignement Supérieur et de la Recherche Scientifique

Université Amar Thelidji- Laghouat

FACULTE: DE TECHNOLOGIE

DEPARTEMENT : D'ELECTRONIQUE

MEMOIRE DE MASTER

Réalisé par : Khadidja Slimanefissa et Hala Guenfoud

DOMAINE : Technologie

FILIERE : Télécommunication

OPTION : Système de télécommunication

Thème

Wideband antenna gain enhancement based on metamaterial for 5G application

Jury de soutenance :

Nom et Prénom	Grade	Qualité
Chaker SALEH	MCB	Encadreur
Chellali Safouane	MAA	Président
Bensafieddine Djalel	MAA	Examinateur

Promotion : 2020/2021

REMERCIEMENT

"كن عالما .. فإن لم تستطع فكن متعلما ، فإن لم تستطع فأحب العلماء ، فإن لم تستطع فلا تبغضهم"

Nous remercions tout d'abord, ***Allah*** *qui nous a donné la force*
Et le courage pour terminer nos études et élaborer ce modeste travail.
Nous remercions Mr l'encadreur ***Cheker*** *qui est bien voulu de nous encadrer, ainsi que pour leur effort et conseils, et aussi pour leur encouragement pendant toute la durée de notre travail, ainsi*
Nous remercions également tous nos enseignants de département d'électronique, université de Ammar Thelidji Laghouat pour l'effort fourni pendant la durée de nos études.
Finalement nous tenons à remercier les membres du jury pour l'honneur de juger notre travail.

اهداء

بسم الله الرحمن الرحيم

﴿ قل اعملوا فسيرى الله عملكم ورسوله والمؤمنون ﴾

الهي لايطيب الليل إلا بشكرك ولا يطيب النهار إلى بطاعتك

ولا تطيب اللحظات إلا بذكرك .. ولا تطيب الأخرة إلا بعفوك ولا تطيب الجنة إلا برؤيتك

إلى من بلغ الرسالة وأدى الأمانة ونصح الأمة إلى نبي الرحمة ونور العالمين سيدنا محمد صلى الله عليه وسلم

إلى نبع الحب والحنان

إلى رمز العطاء وبلسم الشفاء إلى القلب الناصع بالبياض الى من احبها اكثر من نفسي الى من كان دعاؤها سر نجاحي الى ملاك حياتي

(والدتي الحبيبة)

ستبقى كلماتك نجوم أهتدي بها اليوم وفي الغد وإلى الأبد .

الى من كلله الله بالهيبة والوقار .. إلى من علمني العطاء بدون انتظار .. إلى من أحمل اسمه بكل افتخار ابي الحبيب

إلى القلوب الطاهرة الرقيقة والنفوس البريئة إلى ريحانات و لؤلؤات حياتي

(حنان -العالية - خيرة)

الى سندي و قرة عيني اخي و حبيبي بلقاسم

الى من شاركني فرحي وحزني وكان سندي وسر بسمتي خطيبي العزيز مصطفى

إلى الروح التي سكنت روحي جدتي رحمها الله واسكنها فسيح جنانه

الى من اعانني على مصاعب الحياة بالصلاة و الدعوات خالي العزيز مبروك

ولا انسى بالذكر ازواج اخواتي يوسف ومصطفى

الى المدللين فخرو ورانيا

الى مؤنساتي في الاقامة الجامعية (حفصة وعائشة)

الى من تعبت وسهرت معي ، تقاسمت الجهد ، العناء والفرح لانجاز هذا العمل خديجة

هالة

بسم الله الرحمن الرحيم

قل اعملوا فسيرى الله عملكم ورسوله والمؤمنون

الهي لايطيب الليل إلا بشكرك ولا يطيب النهار إلى بطاعتك

ولا تطيب اللحظات إلا بذكرك .. ولا تطيب الأخرة إلا بعفوك ولا تطيب الجنة إلا برؤيتك

إلى من بلغ الرسالة وأدى الأمانة ونصح الأمة إلى نبي الرحمة ونور العالمين سيدنا محمد صلى الله عليه وسلم

إلى من اعطتني الحب والحنان

إلى رمز الحب وبلسم الشفاء إلى القلب الناصع بالبياض (والدتي الحبيبة)

ستبقى كلماتك نجوم أهتدي بها اليوم وفي الغد وإلى الأبد .

الى من كلله الله بالهيبة والوقار .. إلى من علمني العطاء بدون انتظار .. إلى من أحمل اسمه بكل افتخار ابي الحبيب

إلى القلوب الطاهرة الرقيقة والنفوس البريئة إلى ريحانات و لؤلؤات حياتي (حنان - العالية - خيرة)

الى سندي و قرة عيني اخي و حبيبي بلقاسم

الى من شاركني فرحي وحزني وكان سندي وسر بسمتي خطيبي العزيز مصطفى

إلى الروح التي سكنت روحي جدتي رحمها الله واسكنها فسيح جنانه

الى من اعانني على مصاعب الحياة بالصلاة و الدعوات خالي العزيز مبروك

ولا انسى بالذكر ازواج اخواتي يوسف ومصطفى

الى المدللين فخرو ورانيا

الى مؤنساتي في الاقامة الجامعية (حفصة وعائشة)

الى من تعبت وسهرت معي ، تقاسمت الجهد ، العناء والفرح لانجاز هذا العمل خديجة

هالة بسم الله الرحمن الرحيم

قل اعملوا فسيرى الله عملكم ورسوله والمؤمنون

الهي لايطيب الليل إلا بشكرك ولا يطيب النهار إلى بطاعتك

ولا تطيب اللحظات إلا بذكرك .. ولا تطيب الأخرة إلا بعفوك ولا تطيب الجنة إلا برؤيتك

إلى من بلغ الرسالة وأدى الأمانة ونصح الأمة إلى نبي الرحمة ونور العالمين سيدنا محمد صلى الله عليه وسلم

إلى من اعطتني الحب والحنان

إلى رمز الحب وبلسم الشفاء إلى القلب الناصع بالبياض (والدتي الحبيبة)

ستبقى كلماتك نجوم أهتدي بها اليوم وفي الغد وإلى الأبد .

الى من كلله الله بالهيبة والوقار .. إلى من علمني العطاء بدون انتظار .. إلى من أحمل اسمه بكل افتخار ابي الحبيب

إلى القلوب الطاهرة الرقيقة والنفوس البريئة إلى ريحانات و لؤلؤات حياتي (حنان - العالية - خيرة)

الى سندي و قرة عيني اخي و حبيبي بلقاسم

الى من شاركني فرحي وحزني وكان سندي وسر بسمتي خطيبي العزيز مصطفى

إلى الروح التي سكنت روحي جدتي رحمها الله واسكنها فسيح جنانه

الى من اعانني على مصاعب الحياة بالصلاة و الدعوات خالي العزيز مبروك

ولا انسى بالذكر ازواج اخواتي يوسف ومصطفى

الى المدللين فخرو ورانيا

الى مؤنساتي في الاقامة الجامعية (حفصة وعائشة)

الى من تعبت وسهرت معي ، تقاسمت الجهد ، العناء والفرح لانجاز هذا العمل خديجة

هالة ر.

إهـــــــداء

إلى من غرست في المطاف صفحات ووصفت لي من الأمل طرقات،
واختصرت بابتسامتها كل الممرات وفي صلاتها كم أكثرت الدعوات،
وإلى التي لا أستطيع وصفها حتى ولو نفذت مني كل الكلمات.

أمي

إلى من فاق حنانه غزارة الأمطار وتحدى بصبره مرارة الأقدار، تلقى
وتتبع الخطوات رغم طول المشوار.

أبي

إلى دفء البيت وسعادته إلى مصدر أحلامي.

إخوتي

إلى أزهار حياتي أبناء أختاي وإخوتي

الى امي الثانية من لاستبخل علي بنصيحة بشام حورية

إلى أبي الثاني من ساندني كلما اردت الانسحاب وبحلو زبير

إلى هيبة وسمية وبحلو

الى ساعدي الايمن توام روحي بوحلو محمد امين اقول له ها
انا على الدرب وصلت وعلى العهد وفيت

إلى صديقاتي بالإقامة

كل من وسعه صدري ولم تسعه كلماتي أهدي هذا العمل.

خديجة

Abstract

Among the most important metamaterial application in the antenna field we can cite the antenna performances enhancement and size reduction .However, Antenna characteristics wideband's a major objective of metamaterial used in the antenna field. We are interested in this work, with, a novel miniaturized metamaterial unit cell for 5G applications. The new structure is composed of an SRR with four slots, this metamaterial a bandwidth of 52.32% A set of unit cells are periodically associated on a substrate, above amicrostrip antenna with new dual slots in the operating frequency band 27GHz-31GHz. The results show that this metamaterial structure offers some interesting features performances, such as wide bandwidth, which makes the design suitable for 5G systems.

Key words: Metamaterial, 5G, Microstrip bandwidth,.

Résumé

Parmi les applications les plus importantes des métamatériaux dans le domaine des antennes, nous pouvons citer l'amélioration des performances des antennes et la réduction de leur taille. Cependant, les caractéristiques des antennes à large bande constituent un objectif majeur de l'utilisation des métamatériaux dans le domaine des antennes. Nous intéressons à ce travail, avec, une nouvelle cellule unitaire de métamatériau miniaturisée pour les applications 5G. La nouvelle structure est composée d'un anneau extérieur à quatre fentes. Cette unité atteint une bande passante de 52,32 %. Les résultats montrent que cette structure de métamatériau offre des fonctionnalités intéressantes, telles qu'une large bande passante, ce qui rend la conception adaptée aux systèmes 5G.

Mots clés : métamatériau, 5G, bande passante Microstrip.

ملخص

من بين أهم تطبيقات metamaterialفي مجال الهوائي، يمكننا نذكرتحسين الأداء وتقليل الحجم ، ومع ذلك ، فإن خصائص الهوائي للنطاق العريض هدف رئيسي لاستخدام المواد الفوقية في مجال الهوائي. نحن مهتمون بهذا العمل ، مع خلية وحدة جديدة لمادة خارقة مصغرة لتطبيقات G5. يتكون الهيكل الجديد من حلقة خارجية بأربع فتحات ، تحقق هذه الوحدة عرض نطاق ترددي قدره 52.32٪. ترتبط مجموعة من خلايا الوحدة بشكل دوري على ركيزة ، فوق هوائي microstrip مع فتحات مزدوجة جديدة في نطاق تردد التشغيل 27 جيجاهرتز -31 جيجاهرتز. تظهر النتائج أن هيكل المادة الفوقية هذا يقدم بعض ميزات الأداء المثيرة للاهتمام ، مثل النطاق الترددي العريض ، مما يجعل التصميم مناسبًا لأنظمة G5

Table of contents

Table of contents.....I

List of figures.....III

List of tables.....VI

Introduction.....1

Chapter I: Generalities

1.Generalities.....2

1.1.Introduction.....2

1.2. 5G Spectrum Recommendations.....2

1.3.Definition of metamaterials.....2

1.4.Historical points for Metamaterials.....3

1.5.Metamaterial characteristics.....4

1.6.Metamaterial classes.....4

1.7.Microscopic view of split ring resonator (SRR).....8

1.8.Metamaterial applications.....9

1.9.Frequency Selective Surface (FSS).....15

1.10.Conclusion.....17

Chapter II: Effective parameters extraction and optimization of homogenized metamaterials

2.Effective parameters extraction and optimization of homogenized metamaterials..... 19

2.1 Introduction..... 19

2.2 The effective media..... 19

2.3 Effective parameters extraction..... 20

2.4 Design of the homogenization metamaterial..... 21

2.5 Effect of unit cell parameter *wg* on the metamaterial electromagnetic behavior... 22

2.6 Effect of unit cell geometrical Lg on the electromagnetic behavior 25

2.7 Effect of the metamaterial unit cell width *W* 28

2.8 Effect of the substrate thickness *hs* 31

2.9 Conclusion: 34

Chapter III: Microstrip Antenna wideband using metamaterial for 5G application

3.Microstrip Antenna wideband using metamaterial for 5G application 35

3.1 Introduction 35

3.2 The proposed antenna design 35

3.3 Proposed antenna with metamaterial 39

3.4 Conclusion 45

Conclusion 46

Bibliography 47

List of Figures

Figure 1-1 : Unit cell types arranged in space compared to atomic scale in conventional materials. 3

Figure 1-2 : Metamaterial classes. 5

Figure 1-3 : (a).Array of SRR.(b).SRR of 1D and 2D unit cells (c).Re(μ_{reff})(solid blue), Im(μ_{eff}) (dashed red)....8

Figure 1-4 : potential applications. 9

Figure 1-5 : (a) and (b) Square lattice of two rows of copper rods and its transmission spectra. Solid and dashed curves represent respectively the measured and calculated transmission. (c) and (d) Square lattice of two rows of discontinuous copper rods and its transmission spectra. Solid and dashed curves represent respectively the measured and calculated transmission.The air gap e=1.5mm.... 10

Figure 1-6 : a) Schematic representation of the first prototype. (b) Photo of the first prototype composed by an antenna in a foam surrounded by wires with diodes.... 11

Figure 1-7 : rectangular horn antenna (a)-alone (b)-with metamaterial. 12

Figure 1-8 : planar waveguides with double SRR metamaterials. 13

Figure 1-9 : Invisibility cloaks 14

Figure 1-10 : Schematic illustration of Vis-NIR SRR metamaterials as dual transducing mode nanosensor for the detection and identification of biomolecules. 14

Figure 1-11 : Plane FSS with different unit cells. 15

Figure 1-12 : The four major groups of FSS elements 16

Figure 1-13 : Filter types based on FSS (a)-low pass filter (b)-high pass filter(c)-band stop filter (d)-band pass filter 17

Figure 2-1 Composite material with (a) periodic (b) non-periodic structure.... 20

Figure 2-2 metamaterial unit cell (a) wg =0 mm ,(b) 0<wg<w and (c) wg= w mm 21

Figure 2-3 Homogenization of metamaterial real grid. 21

Figure 2-4: Effective permittivity of the metamaterial unit cell for different values of *wg*. (**a**) Real part; (**b**) Imaginary part 22

Figure 2-5:Effective permeability of the metamaterial unit cell for different values of *wg*. (**a**) Real part; (**b**) Imaginary part 23

Figure 2-6: refraction index of the metamaterial unit cell for different values of *wg*. (**a**) Real part; (**b**) Imaginary part 23

Figure 2-7: reflected powers P_r ,and absorbed power p_a for different values of *wg*..... 24

Figure 2-8: transmitted power for different values of wg. 25

Figure 2-9: Metamaterial unit cell with the gap Lg 25

Figure 3-1: Patch antenna details :(a) patch without slots and (b) patch with slots.....36

Figure 3-2: Radiation pattern of the patch antenna with and without slots : (a) - E plane, (b) - H plane. 37

Figure 3-3: Reflection coefficient of the microstrip patch antenna with and without slots. 37

Figure 3-4: Realized gain of the microstrip patch antenna with and withoutslots:.....38

Figure3-5 : Simulated current distribution of antenna with and without slots 38

Figure3-6 :3D Radiation gain patterns calculated at ; (a) 26 GHz , (b) 28 GHz and (c) 29 GHz.....39

Figure 3-7 : Periodic structure of metamaterial.....40

Figure3-8: The proposed antenna with metamaterials.....40

Figure 3-9 Realized gain of the proposed antenna with metamaterial for different spacing *h*.41

Figure 3-10 the spacing S between the elements metamaterial.....41

Figure 3-11 Realized gain of the proposed antenna with metamaterial for different spacing S. 41

Figure: 3-12; Radiation pattern in E plane of the antenna with and without metamaterial.....42

Figure: 3-13: Radiation pattern in H plane of the antenna with and without metamaterial. ...42

Figure 3-14 Return loss (S_{11}), for the patch antenna and the metamaterial patch antenna.....43

Figures 3-15 Calculated realized gain versus frequency.....43

Figure3-16 :3D Radiation gain patterns calculated at ; (a) 26.5 GHz , (b) 28.5 GHz and (c) 29 GHz.....44

List of tables

Table 2-1 metamaterial dimensions..... 22

Table 3-1 Parametric dimensions of the designed antenna..... 36

Table 3-2 Half power beam width $\theta - 3dB$(deg) and realized gain,bandwidth,s11 of the patch antenna with and without slots..... 39

Table 3-3 Half power beam width $\theta - 3dB$(deg) and realized gain,bandwidth,s11 of the patch antenna with and without metamaterial..... 44

Introduction

5G is the latest mobile network that is currently being deployed around the world, stimulating many interesting discussions about the technology and its use case, the field of telecommunications has undergone a great evolution from the first generation 1G to the fourth generation 4G. It is predicted that the fifth generation for future applications. The aim for 5G networks is to be highly efficient and fast, as well as being able to support more users, more devices, more services, and new use cases without a corresponding impact on cost or carbon footprint [1] The advance of the wireless telecommunications networks ought to develop smart antenna systems. For a best quality of service, it is necessary to enhance the antenna performance and the bandwidth also control the radiation pattern of in the desired directions [2]. Metamaterials are not new in telecommunication field, but recent years have seen a particularly strong craze for these materials. Metamaterials are artificial electromagnetic materials engineered to satisfy the prescribed requirements. superior properties as compared to what can be found in nature are often underlying in the spelling of metamaterial [3]

In this project we propose antenna dual U slots with a novel miniaturized metamaterial unit cell the new structure is composed of an outer ring with four slots for 5G application

Our work is divided into three chapters, of which we will give a brief description in the following lines:

The first one presents a state of art of metamaterials, in which definitions, characteristics, examples and applications are introduced. The second chapter is devoted to the effective parameters extraction of homogenized metamaterials. It presents a brief overview of the homogenization of composite materials, and we extract the constitutive parameters (dielectric permittivity magnetic permeability, and refraction index) of the metamaterial unit cell by Fresnel inversion method. We optimized the metamaterial unit cell geometrical in the operating frequency band 26GHz-31GHz

Finally, the chapter 3 is centered on the designing of the dual slots microstrip antenna with new metamaterial unit cell this later is composed of arrangement of unit cell constituted by a single layer superstrate above the antenna to enhance the antenna performance such as main-lobe beam width and enhance the antenna gain.

1. Generalities

1.1. Introduction

5G is a new technology foundation developed to support growing customer demands in terms of speed, diversity and ease. It is expected to increase network throughput and capacity thanks to the massive MIMO system. In this first chapter, we will present a broad overview on the recent developments of the 5th generation. We are then interested in antennas and their characteristics in addition to meet materials and its characteristics. Metamaterial surfaces play a vital role to achieve the surface waves suppression and in-phase reflection, in order to improve the antenna performance specially in the fifth generation (5G) [4], Metamaterial surface is utilized as a reflector due to its in-phase reflection characteristic and high-impedance nature to improve the gain and the bandwidth In this chapter, we will clarify what metamaterial is and report the recent progress on metamaterials. We also summarize the potential applications in areas such as sub-wavelength imaging, antenna design, invisibility cloak, and bio sensing.

1.2. 5G Spectrum Recommendations

The existing Forth generation (4G) communication system (LTE) uses worldwide frequency bands from 2 GHz to 8 GHz with different center frequencies in different countries and the bandwidth needed in 4th generation is around 5 MHz[5]. As per white paper published by Ericsson published on April 2016 [5] and 5G Americas published on August 2015[6], the next generation (5G) is recommended to use two broad classes of the frequency range. The first class belongs to the category of the bands using in the existing 4G communication, there will be a smooth transition from 4G to 5G below 6GHz. However ITU is expected to introduce new bands above 6GHz to around 50 GHz [7].

1.3. Definition of metamaterials

Metamaterials are man-made materials, composed of artificially structured unit cells that are designed of conventional materials and usually (but not necessarily) arranged in periodic fashion [8] The matter is constituted of atoms and molecules see in figure I-1, and is seen by the electromagnetic waves as electric and magnetic dipolar distributions, which are the microscopic sources of the polarization and magnetization phenomenon. Generally, we can cite three microscopic mechanisms of polarization. The first one is electronic polarization. It is related to the modification of the internal charges repartition of each atom or ion. It is constantly present whatever the state of the considered material. The second one is the atomic

or ionic polarization. It concerns the displacements of atoms or ions compared to their equilibrium positions in the crystalline edifice where they belong. The third one is the orientation polarization. It arises when the atomic or molecular dipole moments are oriented under an electric field action. The origin of the microscopic magnetization is the magnetic moments of the microscopic electric currents resulting from the motion and spin of the charged particles present in atoms.

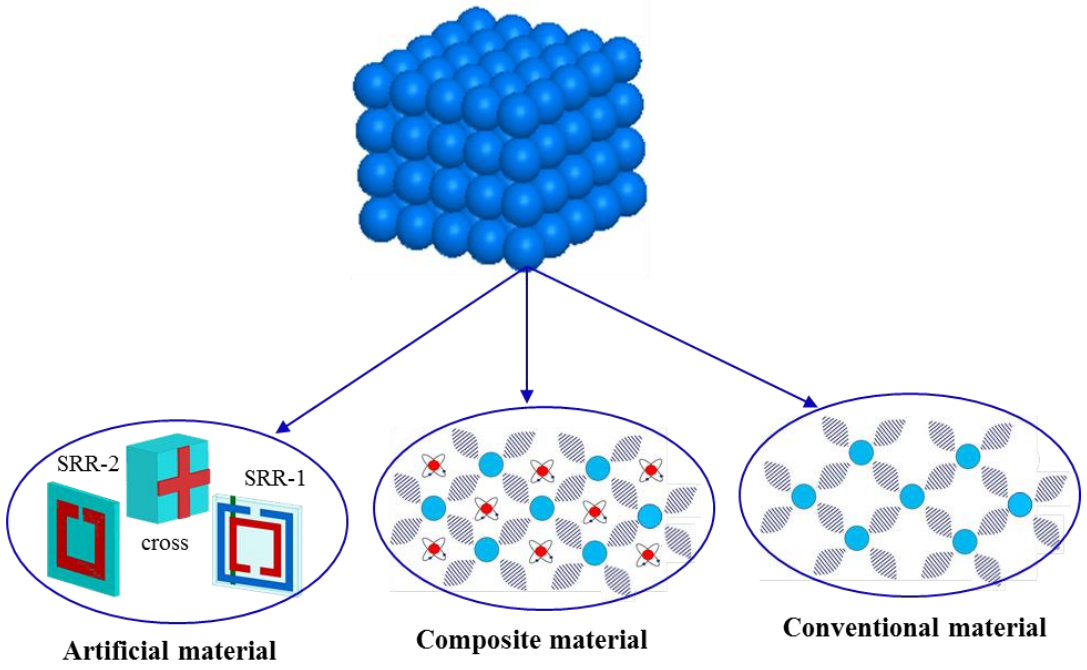

Figure 1-1 : Unit cell types arranged in space compared to atomic scale in conventional materials.

1.4. Historical points for Metamaterials

The word ‘metamaterial’ first appeared in literature in 2000 when Smith et al. published their seminal paper on a structured material with simultaneously negative permeability and permittivity at microwave frequency. Other sources suggest that the term ‘metamaterial’ was first coined by Rodger M. Walser, a physics professor at the University of Texas in 1999.

There are three fundamental papers that should be mentioned in metamaterial history. The first one is Veselago’s paper on left handed materials [9] This paper studied the unusual phenomena to be expected in a hypothetical left handed substance in which the field vectors $\vec{E}$, $\vec{H}$ and the wave vector $\vec{k}$ form a left handed system. The paper also explicitly presented the required material parameters to achieve the material simultaneously negative values of permittivity and permeability. The second one consists of the first experimental demonstration of a Veselago medium by Smith et al. which represents a passage from a theoretical prediction to an experimental validation [10]. The third paper is Pendry’s work on a perfect

lens which represents the initial attempt to fill the gap between novel metamaterials and exciting applications [10].

1.5. Metamaterial characteristics

The structural units of metamaterials can be tailored in shape, size, and the composition. The inclusions composition and morphology can be designed and artificially tuned, and placed in a predetermined manner to achieve prescribed functionalities.

The dependence of metamaterial properties on the unit cell architecture provides great flexibility to control metamaterials electromagnetic responses which are described by the electric permittivity and the magnetic permeability. So, by varying the different unit cell geometry parameters, we can create an agile metamaterial which electromagnetic response is unavailable in nature and can be tailored in practice to a reach desired profile. Metamaterial tailoring is one of the important advantages of metamaterials [11].

1.6. Metamaterial classes

Permittivity ε and permeability μ are two parameters used to characterize the electric and magnetic properties of materials interacting with electromagnetic fields.

The permittivity is a measure of how much a medium changes to absorb electrical energy when it is subjected to an electric field [11-12] It is defined as the ratio of the electric displacement $\vec{D}$ and the electric field $\vec{E}$. The common term dielectric constant is the ratio of permittivity of the material to that of free space ε_0. It is also termed as the relative permittivity. The permeability is also defined as the ratio of the magnetic induction $\vec{H}$ and magnetic field $\vec{B}$. The free-space permeability μ_0 is approximately 1.257×10^{-6} H/m. Recently, Ziolkowski [13-14] has categorized metamaterials by their constitutive parameters as shown in figure 1-2 Most of the materials in nature have positive permittivity and permeability, and hence, they are referred to as ‘double-positive’ (DPS’ medias or right-handed materials (RHM). In contrast, if both of these quantities are negative, these medias are called ‘double-negative’ (DNG) and are also referred to as left-handed materials (LHM). Finally, materials with one negative parameter are named ‘single-negative’ (SNG) and are further classified into two subcategories, namely, ‘epsilon-negative’ (ENG) an ‘mu-negative’ (MNG). Interestingly, natural materials such as cold plasma and silver exhibit negative permittivities at microwave and optical frequencies, respectively, and ferromagnetic materials exhibit a negative permeability behavior in the VHF and UHF regimes. However, to date, no

materials that exhibit simultaneous negative permittivity and permeability have been found in nature, and hence they must be produced artificially.

The first comprehensive review of the history of negative refraction and metamaterials was given by Moroz [15] figure I-2. He indicated that some of metamaterial research started long before Veselago's work and went back to as far as 1905, [16] suggested the existence of backward waves, which are associated with waves in which the phase propagates in a direction opposite to that of the energy flow. Moroz's on-line article first appeared in 2003, tracing the roots of research on backward waves, negative refraction, and LHM. Only recently, Veselago and Narimanov [16] , Shivola [15] , and Shamonina have linked LHMs, and more generally metamaterials, to the earlier works.

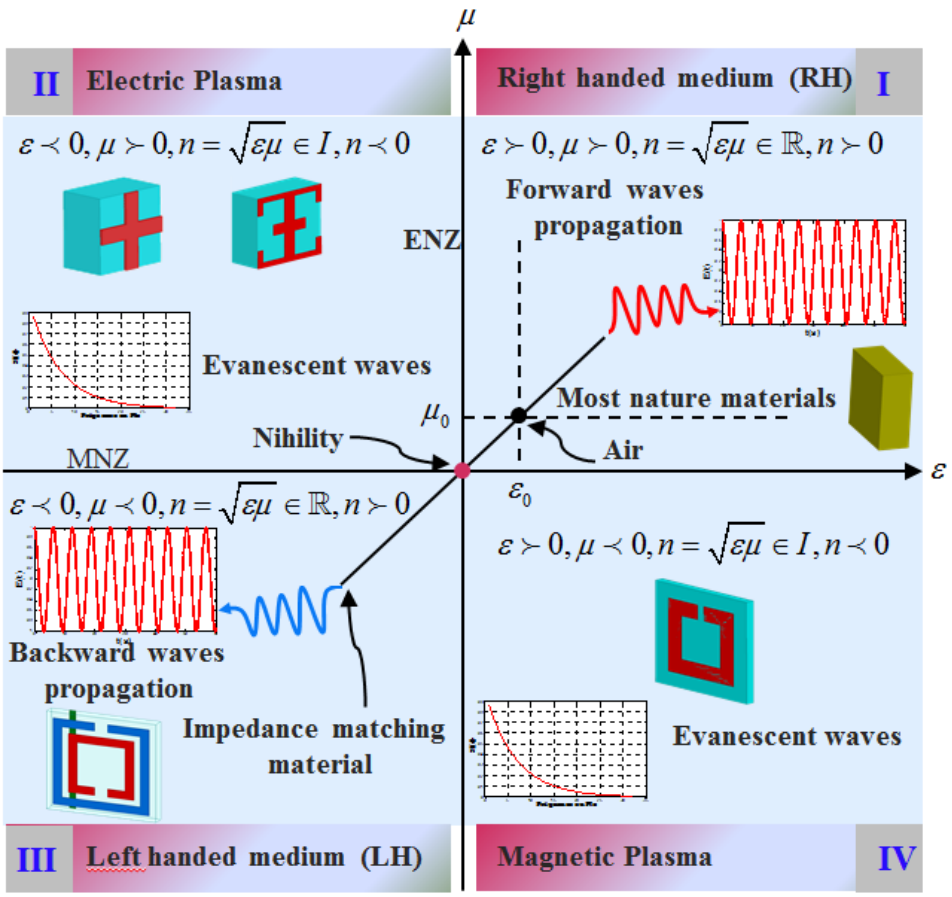

Figure 1-2 : Metamaterial classes.

From figure 1-2 four possible quadrants can be taken:

- Quadrant 1: double-positive media or right-handed materials $\varepsilon \succ 0$ and $\mu \succ 0$.

This quadrant represents (RHM), which support the forward propagating waves. It is well know that the constitutive parameters ε and μ are related to the refractive index *n* by:

$$n = \sqrt{\varepsilon_r \mu_r} \qquad (1\text{-}1)$$

We have $\varepsilon \succ 0 \Rightarrow \varepsilon = |\varepsilon|$ and $\mu \succ 0 \Rightarrow \mu = |\mu|$.

From (1-1) we obtain:

$$n = \sqrt{|\varepsilon_r||\mu_r|} = +\sqrt{|\varepsilon_r||\mu_r|} \qquad (1\text{-}2)$$

$$k = \omega\sqrt{|\varepsilon_r||\mu_r|} = k_0 n \qquad (1\text{-}3)$$

$$\gamma = jk = j\omega\sqrt{|\varepsilon_r||\mu_r|} = \alpha + j\beta \qquad (1\text{-}4)$$

$$\gamma = j\omega\sqrt{|\varepsilon_r||\mu_r|} = \alpha + j\beta \Rightarrow \alpha = 0 \text{ and } \beta = \omega\sqrt{|\varepsilon_r||\mu_r|} = \gamma \qquad (1\text{-}5)$$

We have clearly propagating waves (propagating medium α = 0). The expression of a propagating plane wave in such media is written as:

$$\vec{E} = \vec{E}_0 \exp(-\gamma z) = \vec{E}_0 \exp(-jkz) = \vec{E}_0 \exp(-jk_0 nz) \qquad (1\text{-}6)$$

- Quadrant 2: epsilon-negative medium or electric plasma $\varepsilon < 0, \mu > 0$

In certain frequency regimes many plasmas exhibit this characteristic. For example, noble metals (e.g., silver, gold) behave in this manner in the infrared (IR) and visible frequency domains. This quadrant supports evanescent waves.

We have $\varepsilon \prec 0 \Rightarrow \varepsilon = -|\varepsilon|$ and $\mu \succ 0 \Rightarrow \mu = |\mu|$

From (1-1) we obtain:

$$n = \sqrt{-|\varepsilon_r||\mu_r|} = j\sqrt{|\varepsilon_r||\mu_r|} \qquad (1\text{-}7)$$

$$k = j\omega\sqrt{|\varepsilon_r||\mu_r|} = k_0 n \qquad (1\text{-}8)$$

$$\gamma = jk = j \times j\omega\sqrt{|\varepsilon_r||\mu_r|} = \alpha + j\beta \qquad (1\text{-}9)$$

$$\gamma = j \times j\omega\sqrt{|\varepsilon_r||\mu_r|} = \alpha + j\beta \Rightarrow \beta = 0 \text{ and } \alpha = -\omega\sqrt{|\varepsilon_r||\mu_r|} \prec 0 \qquad (1\text{-}10)$$

And then from (1-7) the expression of a propagating plane wave in such media is written as:

$$\vec{E} = \vec{E}_0 \exp(-\alpha z) \qquad (1\text{-}11)$$

Since α is negative the term $\exp(-\alpha z)$ is divergente when $z \to +\infty$. The evanescent waves are amplified in an ENG media.

- Quadrant 3:double-negative media or left-handed materials $\varepsilon < 0, \mu < 0$

This third case was proposed by Veselago in 1968, supporting the backward propagating waves. We have:

$\varepsilon \prec 0 \Rightarrow \varepsilon = -|\varepsilon|$ and $\mu \prec 0 \Rightarrow \mu = -|\mu|$

From equation (1-1) we obtain:

$$n = \sqrt{-|\varepsilon_r| \times -|\mu_r|} = \sqrt{|\varepsilon_r||\mu_r|} \quad (1\text{-}12)$$

$$k = \omega\sqrt{\varepsilon_r \mu_r} = \omega\sqrt{|\varepsilon_r||\mu_r|} \quad (1\text{-}13)$$

Comparing equations(1-9) and (1-13) then we obtain

$$\alpha = 0 \text{ and } \beta = \omega\sqrt{|\varepsilon_r||\mu_r|} = \gamma \quad (1\text{-}14)$$

Then, the expression of the electric field corresponds to the propagating waves and can be written as:

$$\vec{E} = \vec{E}_0 \exp(-\gamma z) = \vec{E}_0 \exp(-jkz) = \vec{E}_0 \exp(-jk_0 nz) \quad (1\text{-}15)$$

- Quadrant 4: mu-negative medium or magnetic plasma $\varepsilon > 0, \mu < 0$.

In certain frequency regimes some gyrotropic materials exhibit this characteristic. This quadrant supports also evanescent waves.

$\varepsilon \succ 0 \Rightarrow \varepsilon = |\varepsilon|$ and $\mu \prec 0 \Rightarrow \mu = -|\mu|$

From equation (1-1)

$$n = \sqrt{-|\varepsilon_r||\mu_r|} = j\sqrt{|\varepsilon_r||\mu_r|} \quad (1\text{-}16)$$

$$k = j\omega\sqrt{|\varepsilon_r||\mu_r|} \quad (1\text{-}17)$$

From equation (1-9)and (1-17) , we find

$$\beta = 0 \text{ and } \alpha = -\omega\sqrt{|\varepsilon_r||\mu_r|} = \gamma \quad (1\text{-}18)$$

From equation (1-6), the expression of the propagating plane wave in such medium is :

$$\vec{E} = \vec{E}_0 \exp(-\alpha z) \quad (1\text{-}19)$$

Metamaterials have much broader scope than LHM, as shown in figure 1-2. In the $\varepsilon - \mu$ domain, there are several special lines and points indicating special material properties. For

example, the point $\mu = -\mu_0$ and $\varepsilon = -\varepsilon_0$ represents an antiair in the LHM region, which will produce a perfect lens; the point $\mu = 0$ and $\varepsilon = 0$ represents a nihility, which can yield a perfect tunneling effect; the line $\mu = -\varepsilon$ in both RHM and LHM regions represents impedance-matching materials, which have perfect impedance matching with air, resulting no reflections. Also, the vicinity of $\mu = 0$ is called as μ near zero (MNZ) material, and the vicinity of $\varepsilon = 0$ is called as ε-near zero (ENZ) material, which has special properties applied in in perfect lens [16].

1.7. Microscopic view of split ring resonator (SRR)

The SRR in figure I-3-(b) exhibits a permeability frequency response of the form [18]:

$$\mu_{reff}(\omega) = 1 - \frac{\omega_{pm}^2}{\omega^2 - \omega_{0m}^2 + j\Gamma_m\omega} \qquad (1\text{-}20)$$

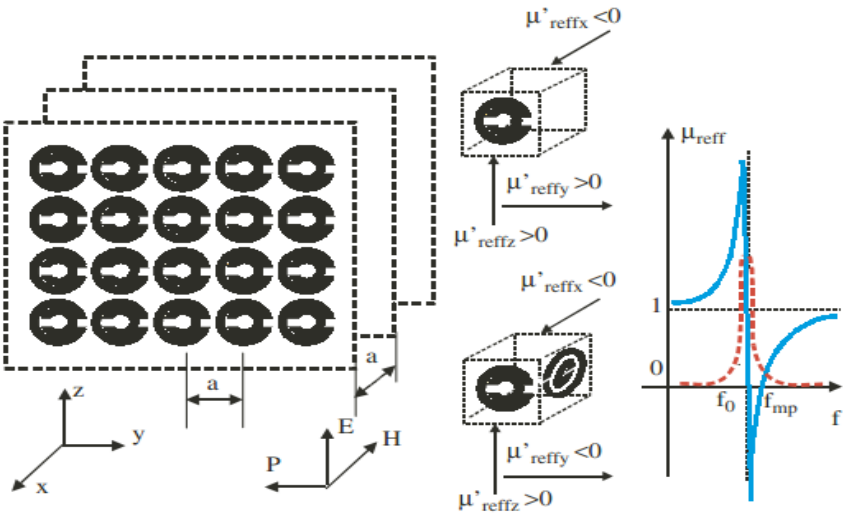

Figure 1-3 : (a).Array of SRR.(b).SRR of 1D and 2D unit cells (c).Re(μ_{reff})(solid blue), Im(μ_{eff}) (dashed red) [14].

Equation (1-20) is divided in real and imaginary parts and presented in figure 1--(c):

$$\mu_{reff}(\omega) = 1 - \frac{F(\omega^2 - \omega_{0m}^2)}{(\omega^2 - \omega_{0m}^2) + (\omega\Gamma_m)^2} + j\frac{\Gamma_m\omega_{pm}^2}{(\omega^2 - \omega_{0m}^2) + (\omega\Gamma_m)^2} \qquad (1\text{-}21)$$

Lorentz parameters are calculated in detail manner in [18]

$$F = \sqrt{\pi(r/a)^2} \qquad (1\text{-}22)$$

$$\omega_{0m} = c\sqrt{\frac{3a}{\pi \ln 2(2wr^3/\delta)}} \qquad (1\text{-}23)$$

Where r, w and δ are the inner radius for the smaller ring, width of the ring and radial spacing between the rings.

We have also:

$$\Gamma_m = \frac{2aR'}{r\mu_0} \qquad (1\text{-}24)$$

R' is the metal resistance per unit length.

We observe from (1-21) that $\mu_{reff} \prec 0$ for $\omega_{0m} \prec \omega \prec = \frac{\omega_{0m}}{\sqrt{1-F}} = \omega_{pm}$

1.8. Metamaterial applications

Due to the exciting and unusual features, metamaterials have found and are finding a lot of applications. Metamaterials can impact on telecommunications, sensing and susceptibility as shown in , across all wave types, but especially electromagnetic and acoustic.

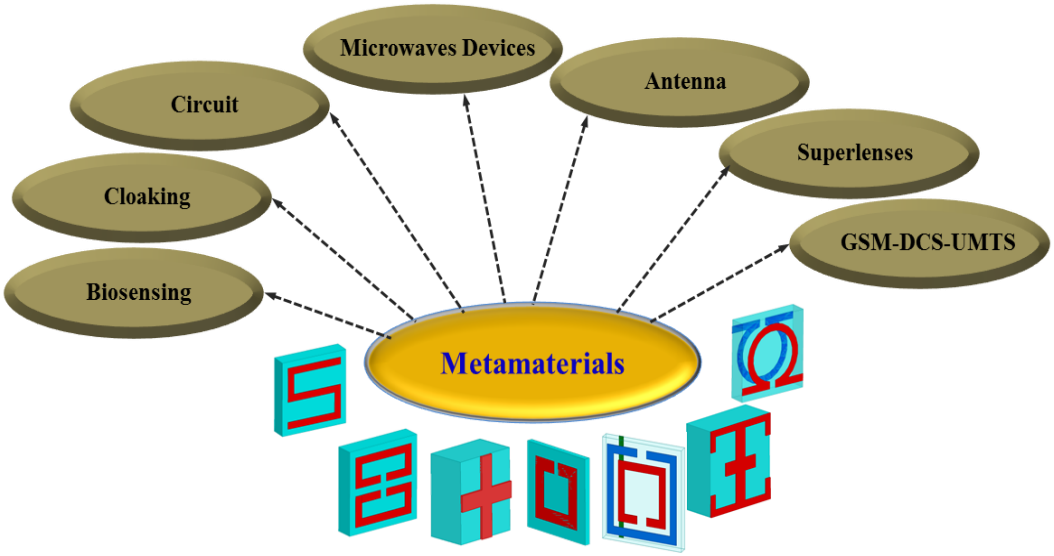

Figure 1-4 : potential applications.

1.10.1. Antenna with a Controllable Metamaterial for Telecommunications

The concept of Controllable photonic band gab (CPBG) or Metamaterial appears with the comparison of the behavior of two complementary passive metallic bidimensional photonic bandgap figure I-5. The first one, which consists of a square lattice of continuous metallic rods figure 1--(a), is well known for having a wide forbidden band from 0 Hz to its plasmon frequency called plasmon-like band figure 1-(b) This last one depends on the geometrical parameters of the structure. In this forbidden band, the effective permittivity is negative [19]. The second one is a square lattice of discontinuous metallic rods figure 1--(c). In this case, Sievenpiper et al. showed that a valence (or transmission) band occurred instead of the plasmon-like band at low frequency figure 1--(d) [20],The effective permittivity becomes positive in this allowed band Some authors have studied this type of lattice.

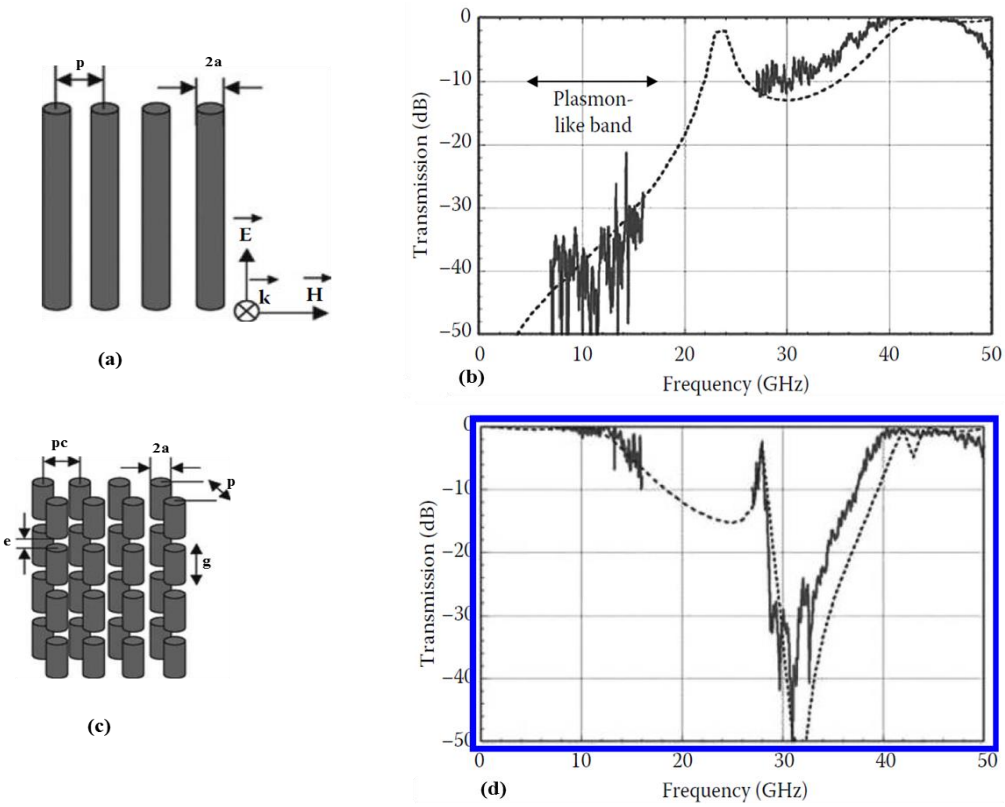

Figure 1-5 : (a) and (b) Square lattice of two rows of copper rods and its transmission spectra. Solid and dashed curves represent respectively the measured and calculated transmission. (c) and (d) Square lattice of two rows of discontinuous copper rods and its transmission spectra. Solid and dashed curves represent respectively the measured and calculated transmission.The air gap e=1.5mm.

The combining antenna with a CPBG was to design a smart antenna for the GSM (900MHz), DCS°(1800MHz), and UMTS (2 GHz) network base station, combine the antenna

and the CPBG to allow the control of the antenna for the three bands, and also to keep a good matching of the antenna with the material.

The CPBG material consists of a multilayer cylindrical array of metallic wires with PIN diodes inserted along them, which surround a wide band antenna. With this kind of configuration, the direction and the magnitude of the radiated power of the antenna can be controlled by "opening" a sector of the lattice with playing with the status of the concerned diodes ON or OFF, Actually, ON state diodes are equivalent to continuous wires while OFF state diodes correspond to discontinuous wires figure 1- represent a first prototype was realized with only one layer of wires and diodes, The discontinuous wires with six diodes are placed on the exterior face of the cylinder and spaced by 15^0. The antenna is inside the structure The upper plate represents the metallic plate with switches to choose which wires of diodes will be ON or OFF. This first prototype validates the possibility to control the beam of the omnidirectional antenna for the three frequency bands But, by using only one layer of wires with diodes figure I-6.

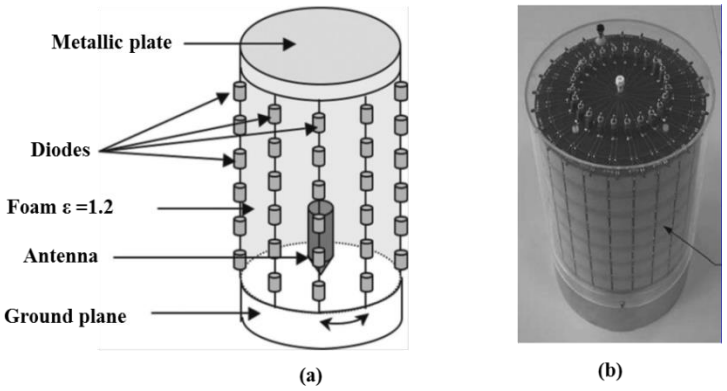

Figure 1-6 : a) Schematic representation of the first prototype. (b) Photo of the first prototype composed by an antenna in a foam surrounded by wires with diodes.

1.10.2. Antennas

Metamaterial antennas are a class of antennas which use metamaterials to enhance or increase the antenna performances. The metamaterial could enhance the radiated power of an antenna. Materials with negative magnetic permeability could possibly allow for properties such as an electrically small antenna size, high directivity, and tunable operational frequency. Furthermore, metamaterial based antennas can demonstrate improved efficiency and high bandwidth performance.

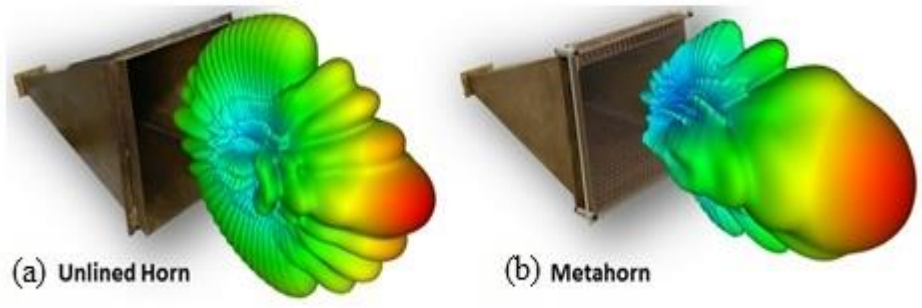

Figure 1-7 : rectangular horn antenna (a)-alone (b)-with metamaterial.

Metamaterials employed in the ground plane surrounding antennas offers improved isolation between radio frequency or microwave channels of (multiple-input multiple-output) (MIMO) antenna arrays. Metamaterial, high-impedance ground planes can also be used to improve the radiation efficiency figure 1-7, and axial radio performance of low-profile antennas located close to the ground plane surface.

Metamaterials have also been used to increase the beam scanning range by using both the forward and backward waves in leaky wave antennas. Various metamaterial antenna systems can be employed to support surveillance sensors, communication links, navigation systems, command and control systems [21].

The gradient refractive index metamaterials are also utilized to produce beam-bending lens and beam-focusing lenses. Based on such properties, high-gain and broadband gradient planar lens antennas and Luneberg-like lens antennas have been proposed and realized [21]. The Industrial, Scientific and Medical (ISM) radio bands are portions of the radio spectrum reserved internationally for the use of radio frequency (RF) energy for industrial, scientific and medical purposes other than communications.

1.10.3. Microwave devices

The waveguided or planar metamaterials which are composed of complimentary structures like CSRR have been used to design microwave components like filters, power dividers, and phase shifters. Narrowband and broadband polarizers have been realized using three-dimensional (3D) anisotropic metamaterial figure 1- [21].

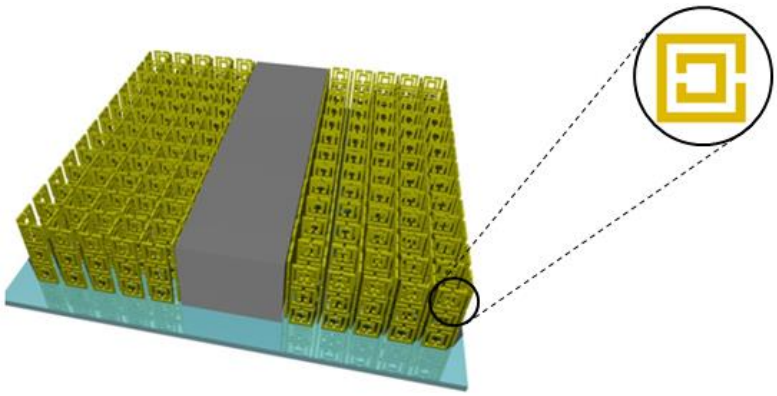

Figure 1-8 : planar waveguides with double SRR metamaterials.

Superconducting metamaterials have been achieved in addition to superconducting split rings and wires. They have been utilized to realize a number of unique applications. The combination of left-handed and right-handed propagation media creates opportunities for new types of resonant structures. By laminating two materials with opposite sense of phase it is possible to create a new class of resonant structures [21]. For example, two flat conducting plates separated by a sandwich of left-handed and right handed metamaterials constitutes such a new resonator. A wave propagating in the direction normal to the plates will suffer a combination of forward and reverse phase windings before reaching the other reflecting boundary. Under these conditions the wave could undergo a net phase shift of 0 radians and still create a resonance condition. The net phase shift could also be a positive or negative multiple of 2π radians as well, each creating a resonant condition. The result is an ultra-compact resonator whose overall dimension is no longer constrained by the wavelength of the resonant wave.

Superconductors are particularly attractive for use in ultra-compact resonators and showed resonances with indices between +2 and -6, including zero, over the broad frequency range from about 5 to 24 GHz [22] Quality factors of the negative order resonances were on the order of 3000 at 30 K, while those for positive order resonances were below 400.

1.10.4. Cloaking

Cloaking devices still attract more and more attention, particularly in the military field. The successful demonstrations of invisible cloaks experimentally in the microwave regime open the possibility to realize cloaking devices [23]. Metamaterials are a basis for attempting to build practical cloaking devices. The cloak deflects microwave rays, so they circumvent the object inside with little distortion figure 1- making it appears almost as if nothing were there

at all. Such a device typically involves surrounding the object to be cloaked with a shell which affects the passage of light near it [23].

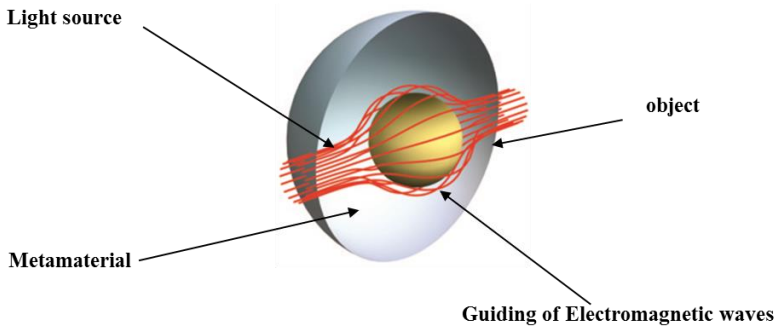

Figure 1-9 : Invisibility cloaks

1.10.5. Biosensing

Another potential application field of metamaterials is on biosensing. Conventional biosensors (such as those based on electro-mechanical transduction, fluorescence, nanomaterials, and surface plasmon resonance) often involve labor-intensive sample preparation and very sophisticated equipment.

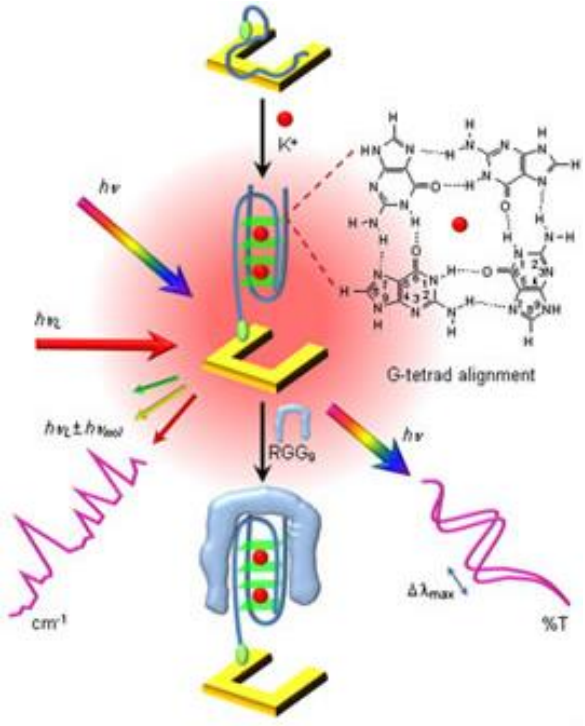

Figure 1-10 : Schematic illustration of Vis-NIR SRR metamaterials as dual transducing mode nanosensor for the detection and identification of biomolecules.

In recent years, researchers have proposed to use metamaterials as candidates for detection of highly sensitive chemical, biochemical and biological analytes. For example, Lee

et al [24] studied the possibility of using split-ring resonators (SRRs) for biosensors. The basic principle is based on the fact that SRR can be considered to be a simple LC circuit with a response frequency of $f = 1/2\pi\sqrt{LC}$, which shows that the resonant frequency varies in terms of the changes in the inductance *L* and/or capacitance *C*. Hence the resonant frequency of the SRR shall be shifted before and after the introduction of biomaterials. Planar metamaterials were proposed to serve as thin-film sensors recently by O'Hara et al [24]. They found that a resonant frequency response can be tuned through metamaterial designs. Though their metamaterial design can only detect thin films having a thickness less than 100 nm, their work presents a promising utlook for THz sensing technology [24].

1.9. Frequency Selective Surface (FSS)

Frequency Selective Surfaces are planar periodic structures of identical patches or apertures of conducting elements duplicate periodically in either a one or two-dimensional array on a dielectric substrate as shown in figure 1-. Because of their frequency selective properties, FSS are incorporated in a wide variety of applications such as the realization of reflector antennas, radome design, making polarizers and beam splitters, and also as radar absorbing structure [24] The frequency behavior of the FSS depends on the shape of the elements (apertures/patches), their size, spacing, and thickness of the metal screen. Generally FSS are employed in front of a grounded dielectric slab (substrate) to synthesize high-impedance absorbing surfaces

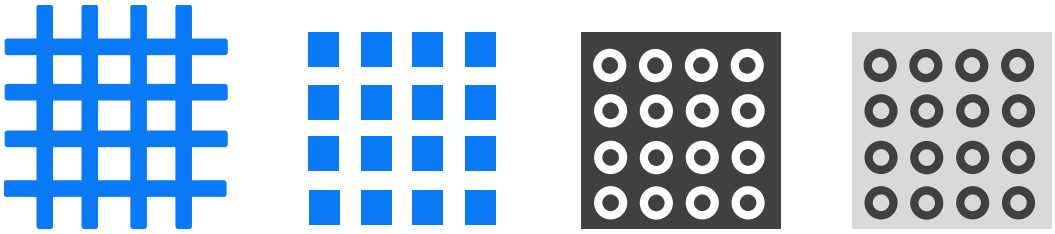

Figure 1-11 : Plane FSS with different unit cells [53-54].

1.11.1. FSS Element Comparison

There are four different types of possible element-type FSS arrays: center connected, loop, solid interior and combination. See figure 1- for some examples of each element type [24].

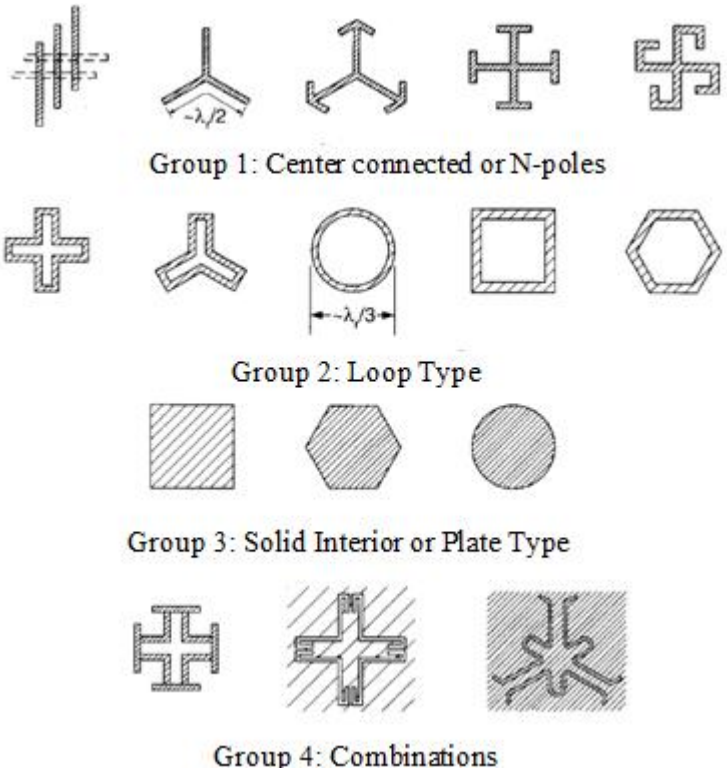

Figure 1-12 : The four major groups of FSS elements [24]

The first group, the center connected elements, are a viable candidate for both radiating and non-radiating arrays. Perhaps the most recognizable from the center connected group is the dipole [24]. The loop elements are in general an excellent choice for non-radiating element FSS arrays. These elements are typically smaller in the *x* and *y* directions than the center connected elements with respect to a wavelength and thus can be spaced close to one another. Plate elements in general do not have very desirable characteristics. First the element have *x* and *y* dimensions around a half of a wavelength, which limits how closely these elements can be placed next to one another. In addition plates are highly inductive elements with small capacitances between them, leading to issues with regard to achieving resonance. If the FSS never resonates, then it is impossible to achieve perfect reflection. This is due to the fact that at resonance, the FSS becomes a short circuit (assuming the materials are lossless) and thus acts as a perfect electric conductor (PEC) ground plane [24] Finally combination elements are too diverse to generalize in any meaningful way. The possibilities in this group are as boundless as the imagination of the designer. Some possible examples of elements in this group have already been shown in figure 1-13 [24]…

The FSS arrays effectively create low pass, high pass, band stop, and band pass filters respectively (see figure 1-) to electromagnetic energy at their design frequency range. These

types of filters are used in a wide variety of applications, including radomes, dichroic surfaces, and circuit analog absorbers [24]..

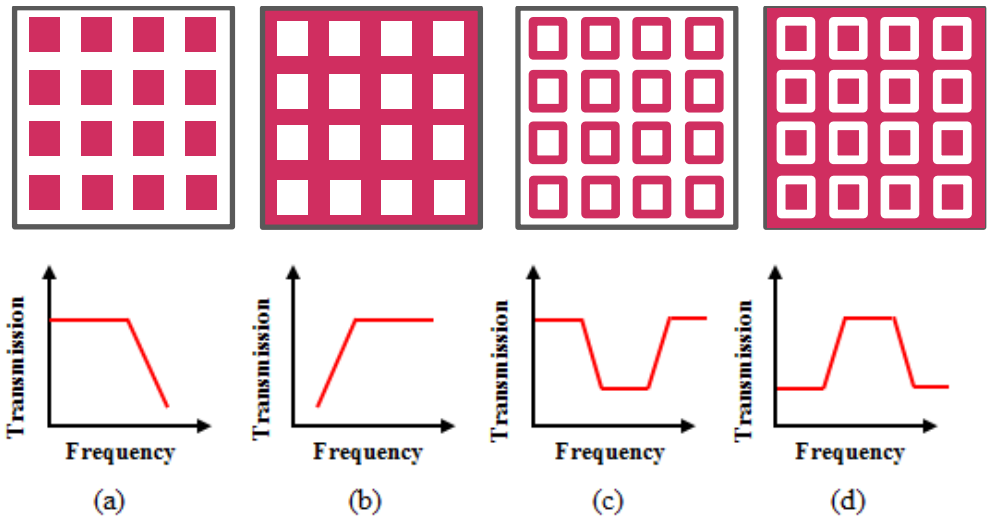

Figure 1-13 : Filter types based on FSS (a)-low pass filter (b)-high pass filter(c)-band stop filter (d)-band pass filter [23].

1.11.2. FSS application

The FSS found their application in:

1- Selective shielding of the electromagnetic interference from high power microwave heating machines adjacent to wireless communication base stations,

2- Selective shielding of frequencies of communication in sensitive areas (military installations, airport, police.),

3- Protection from harmful electromagnetic radiation especially in the 2-3 GHz band in domestic environment, schools, hospitals etc. arising externally (wireless communication base stations) or internally (microwave ovens),

4- Control of radiation at unlicensed frequency bands (Bluetooth applications, 2.45 GHz),

1.10. Conclusion

Metamaterials have contributed a lot in various fields. the field of wireless communication is also not untouched from these highly engineered materials. metamaterials have the capability to control the electromagnetic property

This metamaterials are artificial materials, their electromagnetic responses, which are the effective dielectric permittivity and effective magnetic permeability can be tailored and designed in request. These characteristics allow metamaterials to be useful. Consequently,

metamaterials including FSS have many applications in different frequency domain such as: antennas, microwave devices

2. Effective parameters extraction and optimization of homogenized metamaterials

Introduction

The different applications and expected uses of metamaterials in electromagnetic engineering require a precise knowledge of their electromagnetic properties. So the metamaterial homogenization is an important step in the design process, because it is related to the environmental scale and to the effective medium nature (isotropy, chirality …)..

This chapter introduces the metamaterials homogenization and the brief view of the method extraction of metamaterial and finally we characterized and optimized of metamaterial unit cell this to design a metamaterial lens [27]

The effective media

Most electromagnetic phenomena are governed by Maxwell's equations, which are a set of equations describing the interaction between fields, sources, and material properties. Impinging fields in a system can influence the organization of electric and magnetic dipoles in a medium. Fields can induce polarization and magnetization to some degree, depending on the particular material involved. The electromagnetic properties of a material are described by two material parameters: the dielectric permittivity □ and the magnetic permeability□, which characterize the coupling between the material and the electric and magnetic field components, respectively. These two parameters, along with other values, which are the refractive index $n = \sqrt{\mu\varepsilon}$ the impedance $Z = \mu / \varepsilon$, are essentially macroscopic effective parameters [28].

Similarly, the scale of in homogeneities in a metamaterial is much smaller than the wavelength of interest. The inhomogeneity scale corresponds to the lattice constant of the artificial structure for the case of periodic metamaterial as shown in figure 2-1.

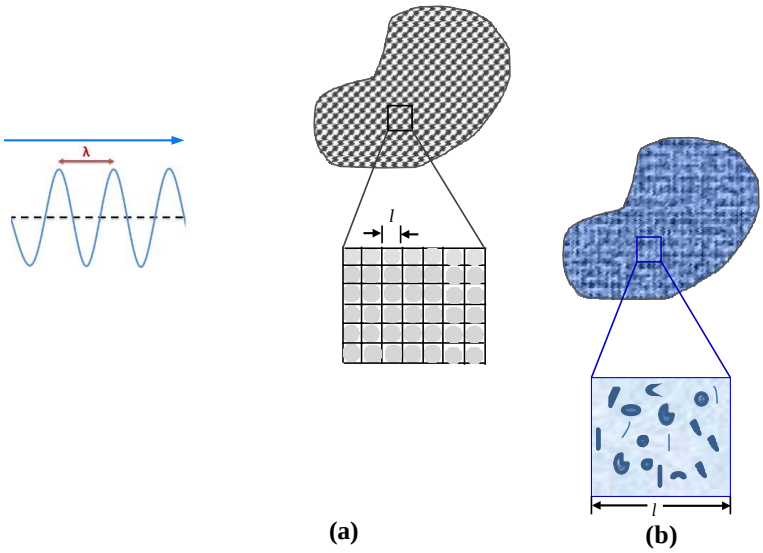

Figure 2-1 Composite material with (a) periodic (b) non-periodic structure

In figure 2-1, the largest heterogeneity length scale l should be small enough compared to the smallest length scale λ that is of physical importance. For a periodic medium (in the left of the figure) l is the unit cell size while in a random medium (in the right of the figure) it should be the smallest size of a sphere which at any position is a statistical representative of the entire body.

Then the key of homogenization is when the size of the unit cell is much smaller than the operating wave length [29-30] This property is called the homogenization criterion. Since the metamaterial can be seen as an homogeneous medium.

Effective parameters extraction

If the size of the metamaterial unit cell is much smaller than the operating wave length, so we can consider that the metamaterial is homogenous and it responds to electromagnetic waves in a similar way [31]. It is possible to describe the metamaterials as continuous materials. In these conditions, they can be characterized by effective parameters without considering the local field distribution. This part of the chapter treats classical and numerical homogenization approaches, which are the S parameters extraction method (Fresnel inversion method) and the field summation method which is an averaging approach

The metamaterial effective parameters extraction requires two steps [32-33]

1- Computation of the homogenized metamaterial forward and backward wave impedance (z^+, z^-) and complex refractive index (n) which are expressed in terms of reflection and transmission coefficients (S_{ij}).

2- Retrieval of the electromagnetic constitutive parameters (permittivity, permeability)

from the S_{ij} parameters.

Design of the homogenization metamaterial

In this section, we design a planar metamaterial unit cell shown in figure 2-3 consists of an outer ring with four capacitive slots with width wg, the gap wg can be optimized to obtain *the* metamaterial is a periodic arrangement has two equal periods ***a*** in the *x* and *y* directions as shown in figures 2-3 The unit cell is made of dielectric substrate type of Rogers RT/Duroid 5880 with a relative permittivity of 9.2 and dielectric loss tangent of 0.002.

And a thickness ***d*** and metallization thickness *t* which has a length ***L*** such as ***L*** < *a*, a width ***w***

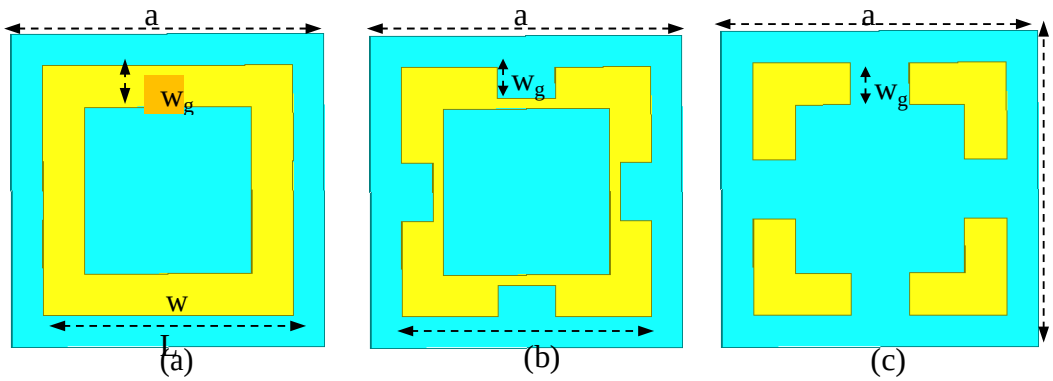

Figure 2-2 metamaterial unit cell (a) wg =0 mm ,(b) 0<wg<w and (c) wg= w mm

The effect of the gap w_g can be designed three stricture when wg=0, we obtain the square metamaterial unit cell without gab figure 2-4 (a) , and for 0<wg<w we obtain strectur (b) and finaly for the wg=w we obtain another stricture metamaterial unit cell figure 2-4 (c)

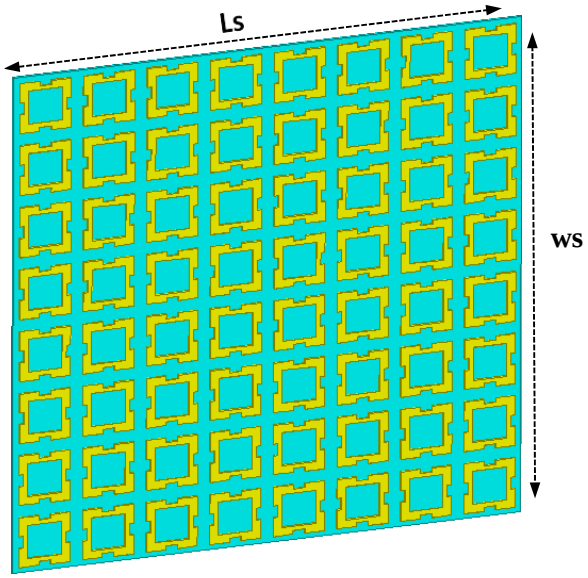

Figure 2-3 Homogenization of metamaterial real grid.

Effect of unit cell geometrical parameter *wg* on the metamaterial electromagnetic behavior

In this section we examine the influence of the gap w_g of the metamaterial unit cell

On the electromagnetic behavior of the metamaterial represented by the constitutive parameters (ε_{eff}, μ_{eff}) and refraction index *n*. The unit cell geometrical parameters are: the metallization thickness *t*, the conductor width *w*, the gap w_g and the substrate thickness *d*.

The dimensions of the metamaterial unit cell are represented in table 2-2.

Table 2-1 metamaterial dimensions

parametres	Dimension (mm)	parametres	Dimension (mm)
d	12	a	1.5
w	0.2	Ls	12
t	0.035	Ws	12
L	1.2	wg	opt

The simulation results of the electromagnetic parameters (μ_{eff} and ε_{eff}) of the metamaterial unit cell for different values of the gap Wg using Fresnel inversion method [33] are shown in figure2-4 and 2-5

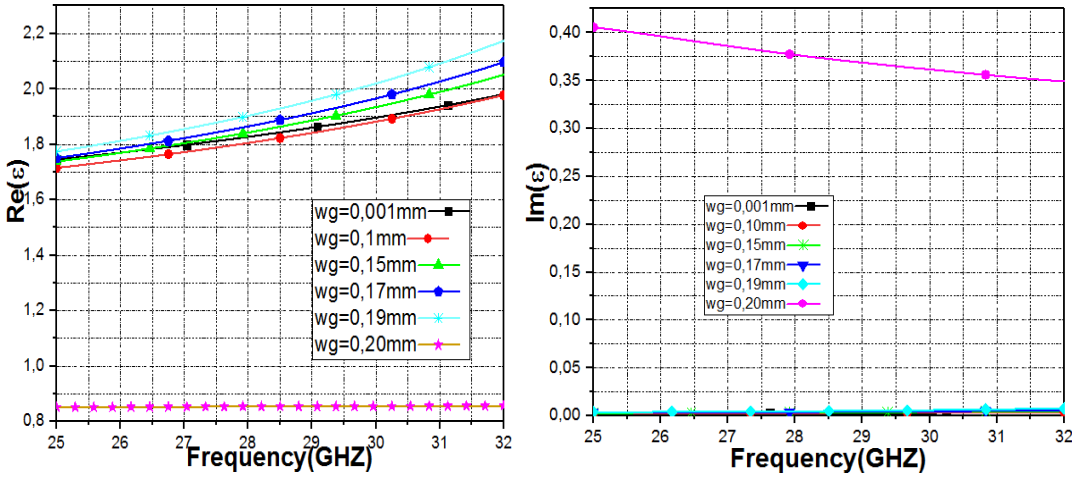

(a) (b)

Figure 2-4: Effective permittivity of the metamaterial unit cell for different values Of *wg*. (**a**) Real part; (**b**) Imaginary part

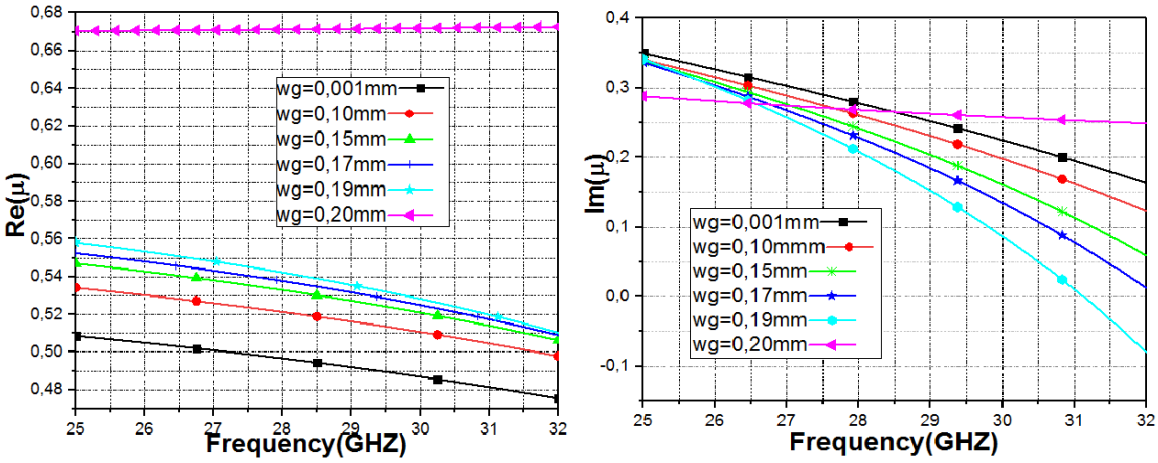

(a) (b)

Figure2-5:Effective permeability of the metamaterial unit cell for different values Of *wg*. (**a**) Real part; (**b**) Imaginary part

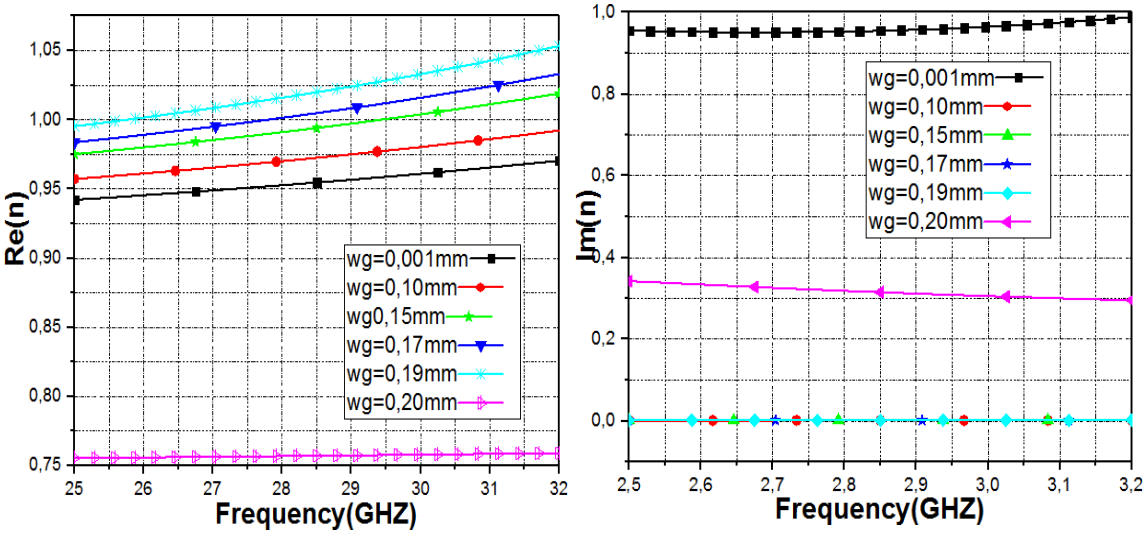

(a) (b)

Figure2-6: refraction index of the metamaterial unit cell for different values Of *wg*. (**a**) Real part; (**b**) Imaginary part

from figure 2-4 it can be seen that the imaginary of the permittivity near to zero for the wg<w correspond the two structure (a) and (b) and for the structure (c) the imaginary part near to 0.4mm and the real part between 0.8 and 1.8, and the imaginary part of the permeability is lower than 0.4 and the real part between 0.5 and 0.68

And from figure 2-6 it can be seen the real and imaginary part of the refractive index of the metamaterial unit cell are near to zero for the values $0.1 \leq wg \leq 0.19$

Figures 2-7 and 2-8 illustrate the effect of the gap w_g on the absorbed Pa, reflected Pr, and transmitted Pt powers in the conductor based on the metamaterial unit cell

Figure 2-7 (b) shows that the absorbed and reflected powers in the metamaterial corresponding to wave propagation in the forward directions; are slightly different and decrease when we increase wg. This difference comes from the reflection asymmetry ($S_{11} \neq S_{22}$). For example,. Indeed, for the metamaterial unit cell, the path of the reflected waves (the waves are almost reflected by the conductor strip).

And observe that the maximum absorbed power in the forward direction, corresponding to the structure 3 with wg= 0.2mm and for the wg<0.2 the absorbed power near is to zero and for the reflected power it can be seen that the maximum refracted power for wg<02 mm

And for wg=0.2mm the reflected power near to zero

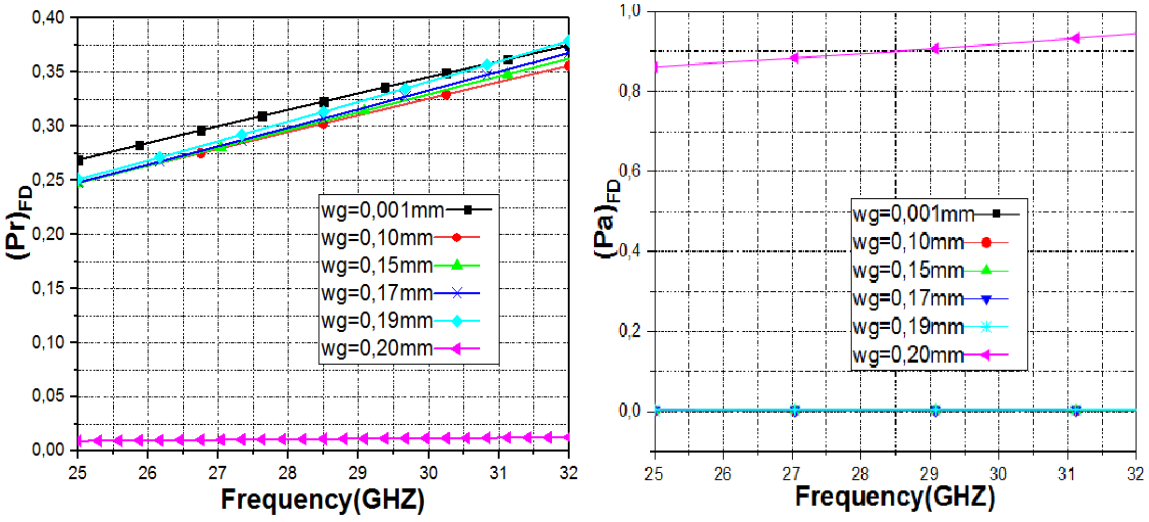

(a) (b)

Figure 2-7: reflected powers P_r ,and absorbed power p_a for different values of *wg*.

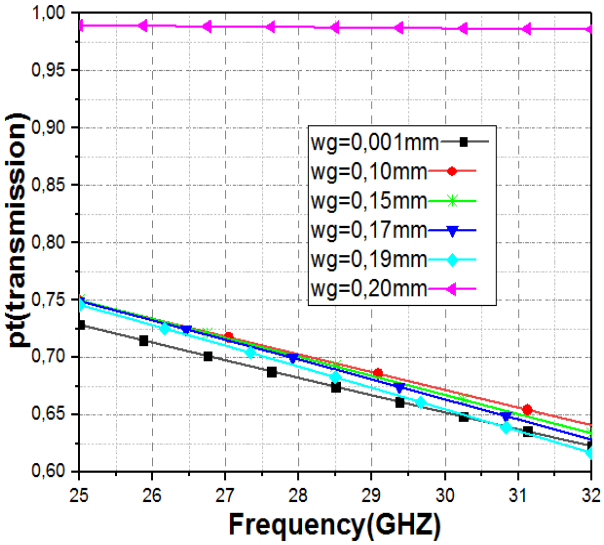

Figure 2-8: transmitted power for different values of wg.

Through the simulation results, we notice that the optimum value when the gap Wg is (0.001mm) corresponding to the absorbed power near to zero and the reflected power about (0.25%) and the transmitted power about 70%

Now we will fixed all the parameters of the metamaterial unit cell and, we can study the effect the gap L_g to see it's effect in the electromagnetic parameters and the powers of the metamaterial

The gap Lg is shown in figure 2- 9,

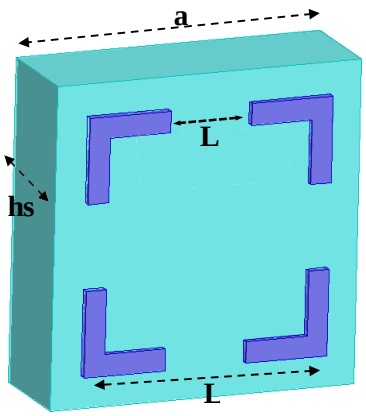

Figure 2-9: Metamaterial unit cell with the gap Lg

Effect of unit cell geometrical parameter Lg on the metamaterial electromagnetic behavior

In this section we study the influence of the gape Lg on the electromagnetic properties of the metamaterial. First, we have fixed the substrate thickness at hs = 0.058 mm and conductor width w = 0.2 mm Secondly, we chose for the gap Lg values available in the data sheet: 0 mm, 0.5 mm and with the step 0.1 mm

We use the Fresnel inversion method to obtain the constitutive parameters (ε_{reff} and μ_{reff})

and the refraction index of the metamaterial.

The simulation results of the electromagnetic parameters (μ_{eff} and ε_{eff}) of the metamaterial unit cell for different values of the gap Lg are shown in figures 2-10 and 2-11

From figure (2-10) it can be seen that imaginary part of the permittivity near zero for Lg=0mm correspondent to the structure A, and for Lg>0mm the imaginary part between 0.5 and 0.68 , and the real part near to the unity for Lg>0 and near to 1.8 for Lg=0mm.

And from figure (2-10) the real part of the permeability is lower than 0.7 for Lg> 0 and near to 0.5 for Lg=0mm, the imaginary part between 0.25and 0.40

And from figure (2-12) it can be seen the real and imaginary part of the refractive index of the metamaterial unit cell; the imaginary part near to zero for the Lg = 0mm between 0.25 and

The real part near to the unity

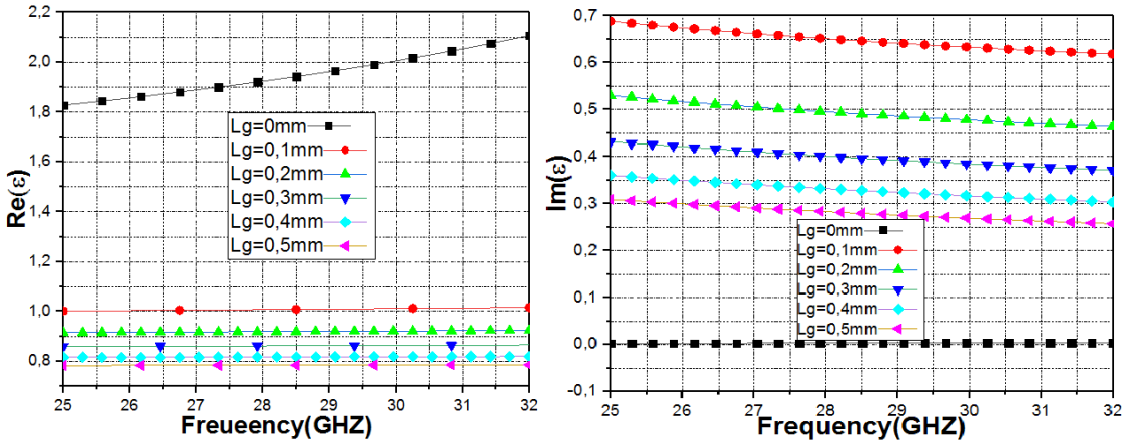

(a) (b)

Figure2-10:Effective permittivity of the metamaterial unit cell for different values Of (*Lg)* (**a**) Real part; (**b**) Imaginary part

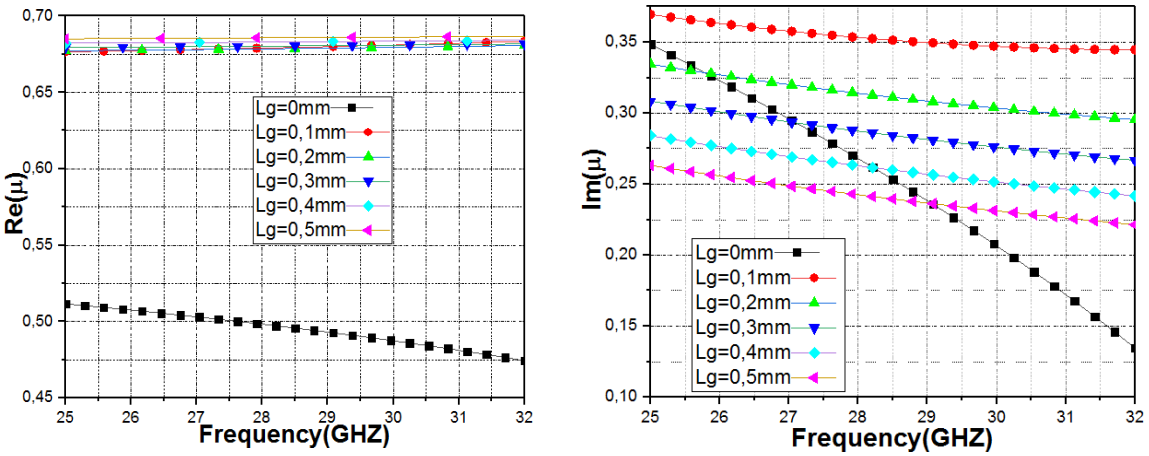

(a) (b)

Figure 2-11: Effective permeability of the metamaterial unit cell for different values Of *Lg*. (**a**) Real part; (**b**) Imaginary part

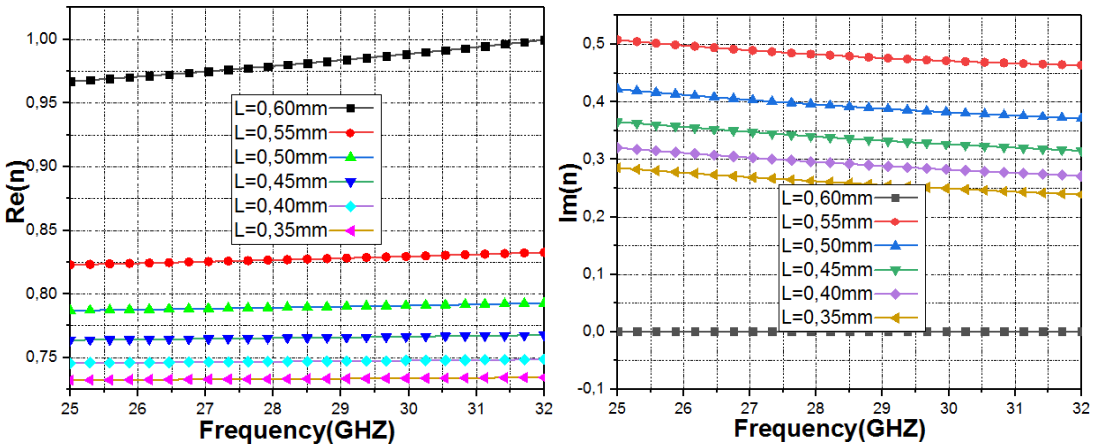

(a) (b)

Figure 2-12: refraction index of the material unit cell for different values of *Lg*

. (**a**) Real part; (**b**) Imaginary part

Figures 2-13 illustrate the effect of the gap Lg on the Absorbed Pa, reflected Pr, and transmitted Pt powers in the gap Lg of the metamaterial, we observe that the maximum absorbed power in the forward direction, when Lg> 0.3mm and for the Lg ≤0.3mm the absorbed power near to zero and the maximum refracted power reflected power found for Lg=0mm, and for Lg>0mm the reflected power near to zero

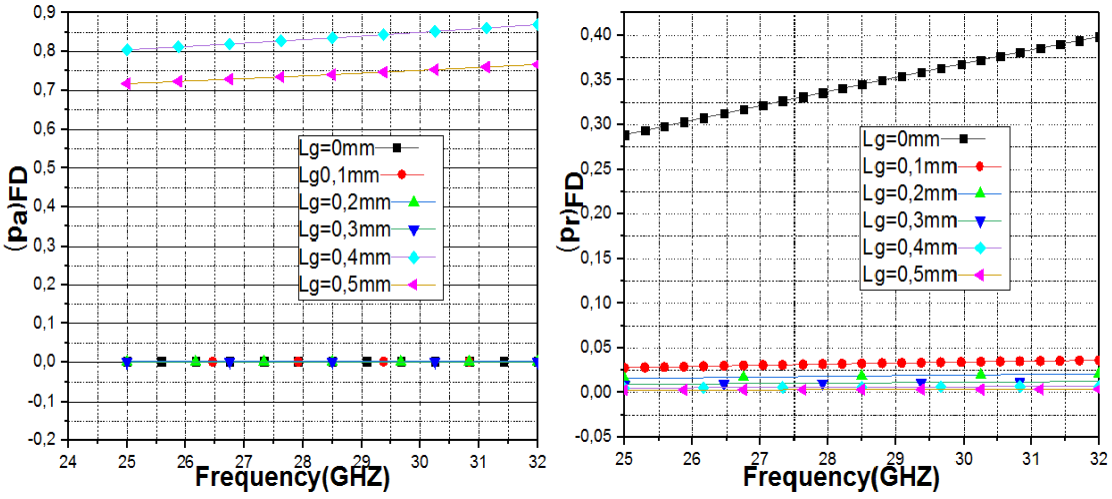

Figure 2-13: powers Pr, and absorbed power p_a for different values of *Lg*.

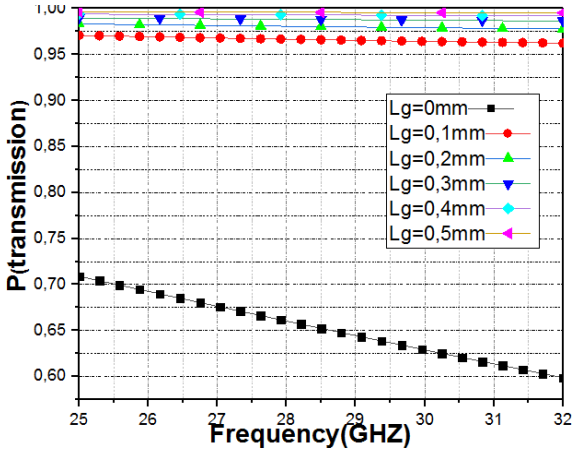

Figure2-14: transmitted power for different values of *Lg*

Through the simulation results, we notice that the optimum value of Lg is (0.1mm) because the reflect power low about (0.30) and the absorbed power near to zero and the transmitted power is 98%

Now all the parameters of the metamaterial unit cell are know, we can also study the effect of the width of the conductor *w* to see it's effect in the electromagnetic parameters and the powers of the metamaterials unit cell with the optimal value of Lg = 0.1 mm.

Effect of the metamaterial unit cell width *W* on the metamaterial electromagnetic behavior

In this section we fixed the value of gap Lg =0.1mm, and we investigate the influence of the conducting width (*w)*in the electromagnetic properties of the met material. We vary the conducting width *w* from 0.05(mm) to 0.3 (mm).

The simulation results of the electromagnetic parameters (μ_{eff} and ε_{eff}) of the metamaterial unit cell for different values of the gap Lg are shown in figures 2-15 and 2-17

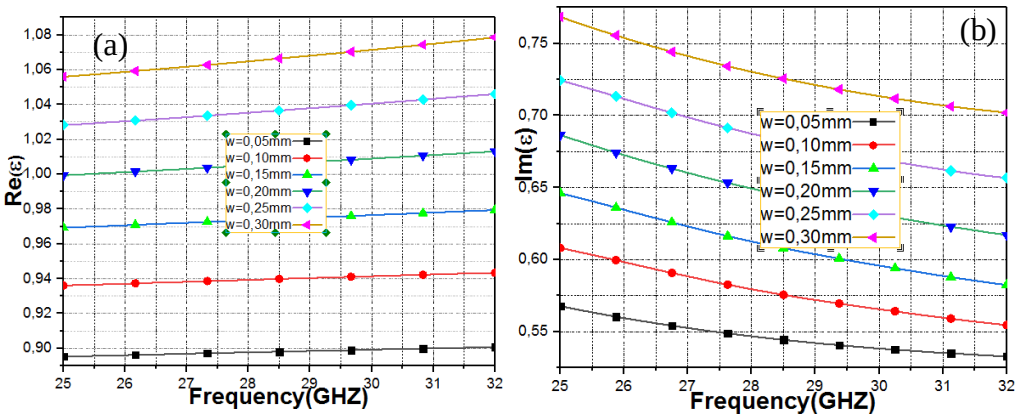

Figure 2-15:Effective permittivity of the metamaterial unit cell for different values

Of *w*. (**a**) Real part; (**b**) Imaginary part

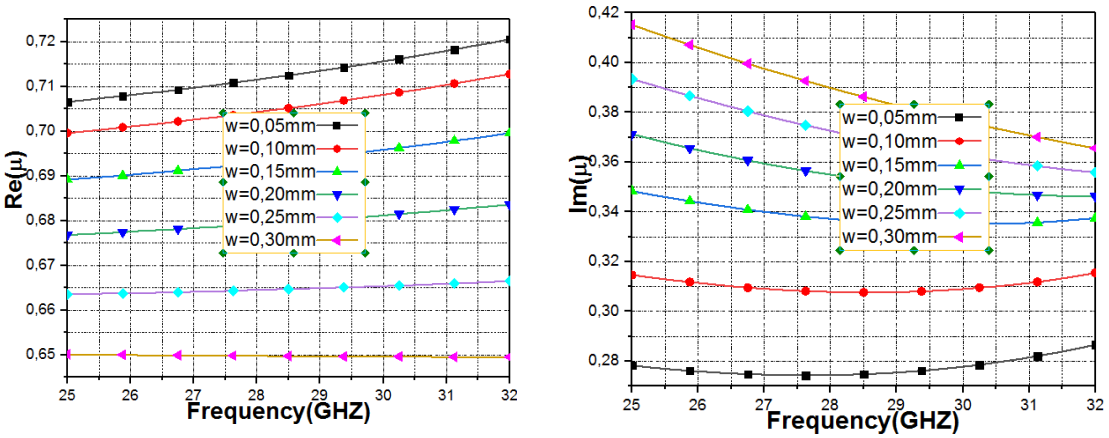

(a) (b)

Figure 2-16: Effective permeability of the metamaterial unit cell for different values Of *w*. (**a**) Real part; (**b**) Imaginary part

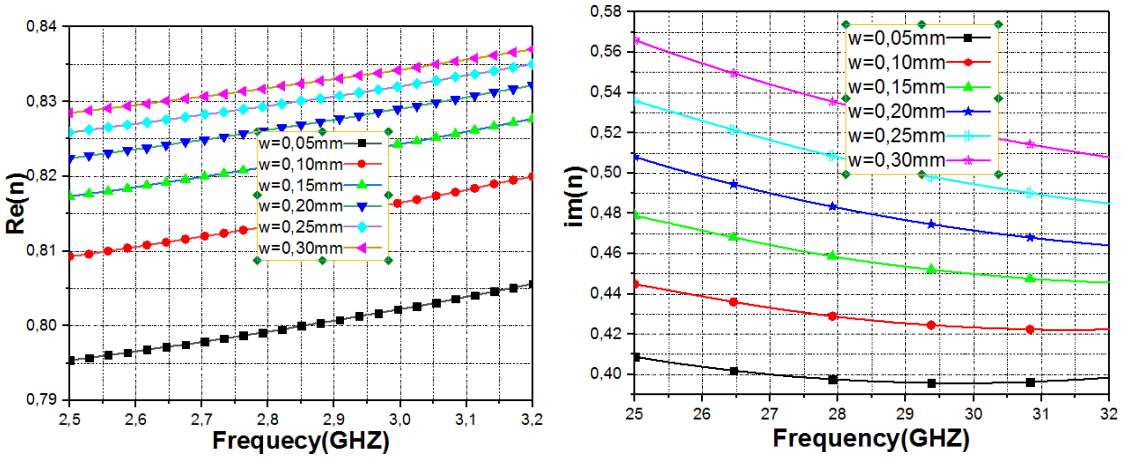

(a) (b)

Figure 2-17: refraction index of the metamaterial unit cell for different values Of *w*. (**a**) Real part; (**b**) Imaginary part

From the figure (2-15) it can be seen that imaginary part permittivity between 0.55 and 0.77 and the real part between 0.85and 1.06 and figure (2-13) shown the imaginary part of the permeability between 0.28.and 0.42; and the real part between 0.65 and 0.71

And figure 2-15 shown the real and imaginary part of the refractive index of the met material unit cell , the real part near to the unity and the imaginary part between 0.40and 0.58 for the values $0.05 \leq w \leq 0.30$.

Figures 2-18 and 2-19 illustrate the effect of the width w on the absorbed Pa, reflected Pr, and transmitted Pt powers in the conductor based metamaterial we observe that the maximum absorbed power in the forward direction, with w<0.05mm and for the w<0.05mm the absorbed power near to zero and for the reflected power figure 2-15 it can be seen that the maximum refracted power for w=0.04mm and for w=0.05mm the reflected power near to zero.

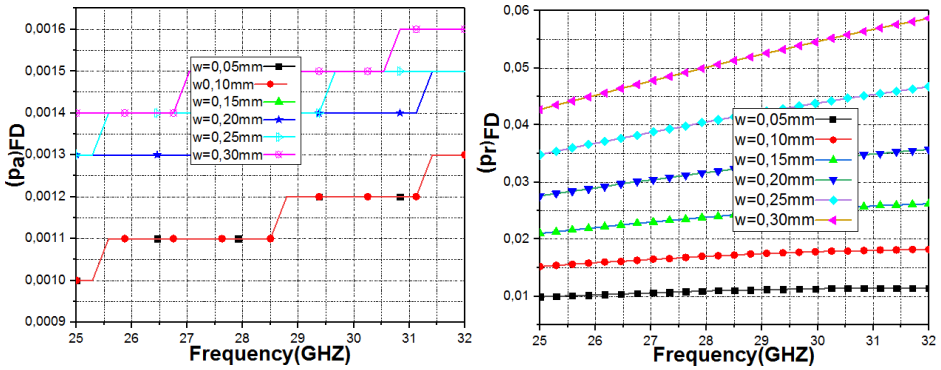

Figure 2-18: powers P_r, and absorbed power p_a for different values of *w*.

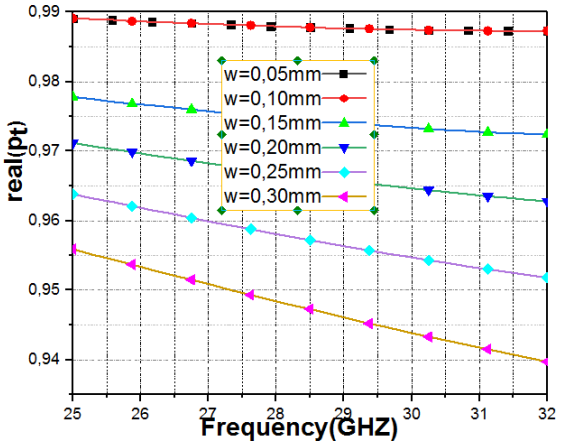

Figure 2-19: transmitted power for different values of *w*

Through the simulation results, we notice that the optimum value of w is (0.1mm) because the reflect and the absorbed power near to zero in the operating frequency band 25GHz -31GHz and the transmitted power is 98%

The substrate thickness *hs* is another parameters cans be optimized to and see its effect on the electromagnetic parameters of the metamaterial unit cell

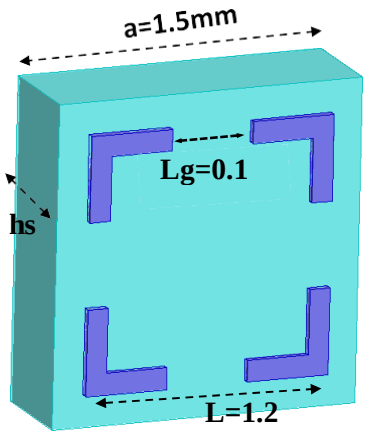

Figure 2-20 : Metamaterial unit cell with hs

Effect of the substrate thickness *hs*

In this section we fixed the all the values (w, t, Lg, a, L) and we investigate the influence of the substrate thickness *hs* in the electromagnetic, the simulation results of the electromagnetic parameters (μ_{eff} and ε_{eff}) and the refraction index of the metamaterial unit cell for different values of thickness hs are shown in figures 2-21 to 2-23.

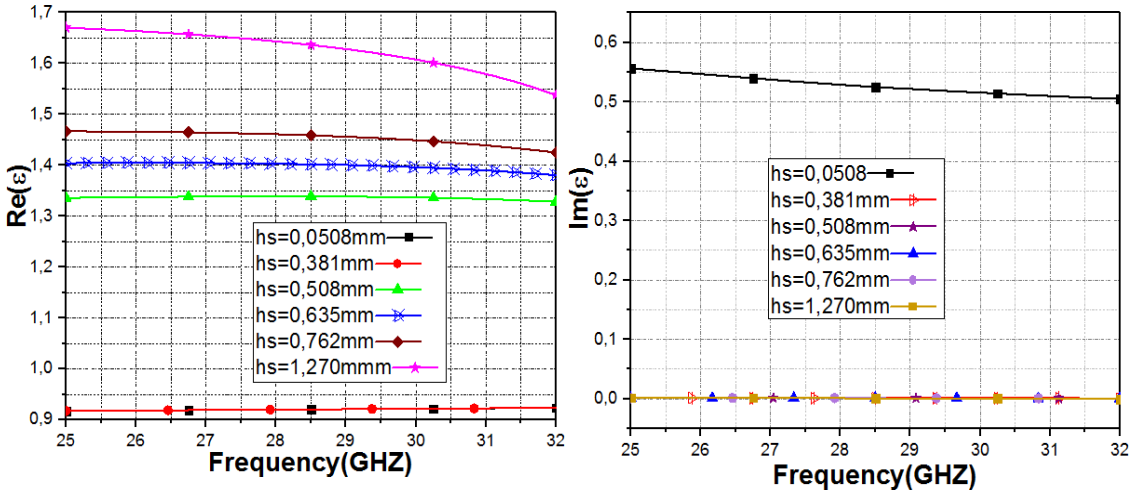

(a) (b)

Figure 2-21: Effective permittivity of the metamaterial unit cell for different Of *hs* (**a**) Real part; (**b**) Imaginary part

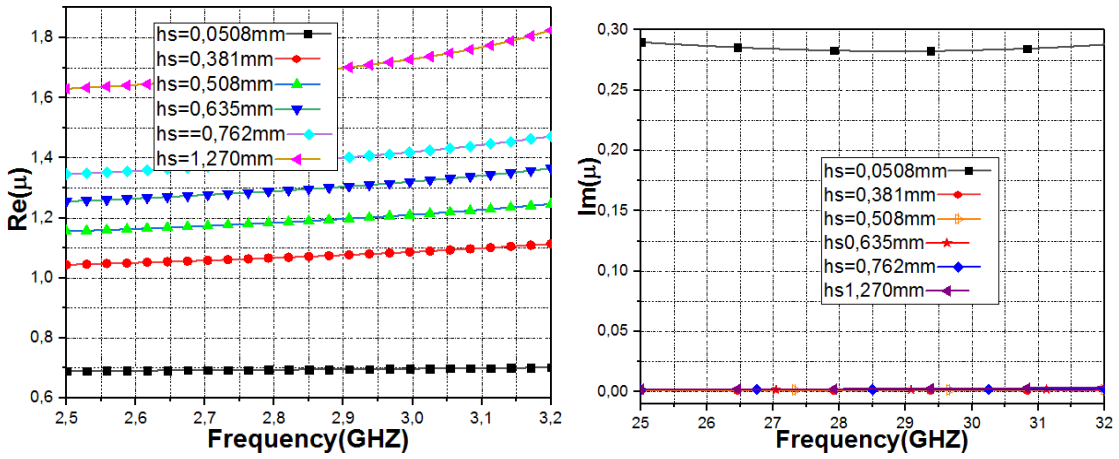

(a) (b)

Figure 2-22:Effective permeability of the metamaterial unit cell for different values of *hs*. (**a**) Real part; (**b**) Imaginary part

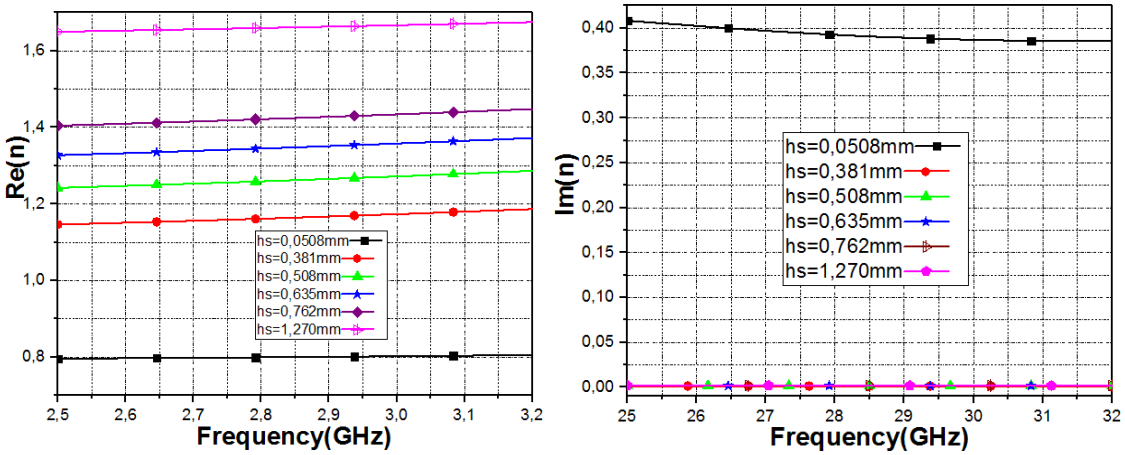

(a) (b)

Figure 2-23 : refraction index of the metamaterial unit cell for different values Of *hs*. (**a**) Real part; (**b**) Imaginary part

From figure 2-17 it can be seen that the imaginary of the permittivity near to zero for the hs > 0.0508mm and for hs =0.0508 the imaginary part near to 0.4 ,and the real part between 1.1 and 1.7 for hs>0.381 and near to zero for the hs=0.0508mm and 0.381mm

From figure 2-18 the imaginary part of the permeability near to zero for the hs<0.0508mm and the real part between 0.7and 1.7

And from figure 2-19 it can be seen the real and imaginary part of the refractive index of the metamaterial unit cell, the real part near to the unity and the imaginary part near to zero for the values $0.381 \leq hs \leq 1.270$

Figures 2-24-2-25 illustrate the effect of the hs on the Absorbed Pa, reflected Pr, and transmitted Pt powers in the conductor based metamaterial

We observe that the maximum absorbed power in the forward direction, with *hs*=1.270mm and for the *hs*<1.270mm the absorbed power near to zero and the maximum refracted power for *hs*=0.0508mm and for *hs*>0.0508mm the reflected power near to zero

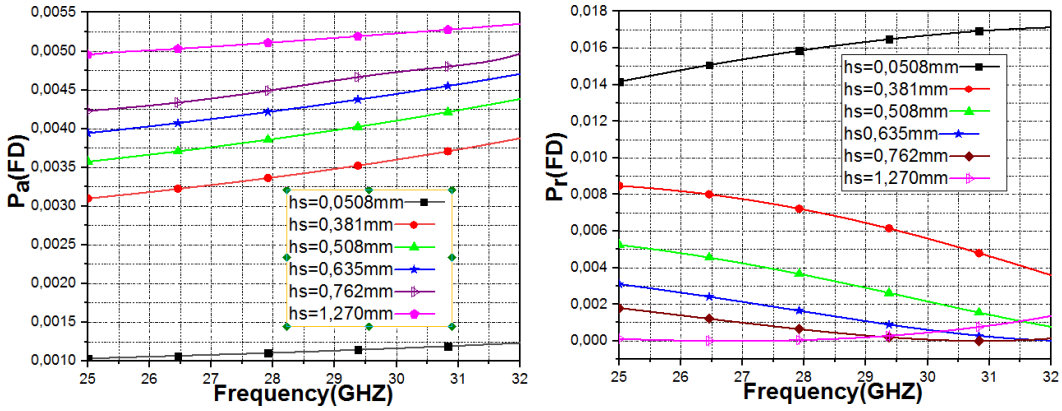

Figure 2-24: powers P_r ,and absorbed power p_a for different values of *hs*

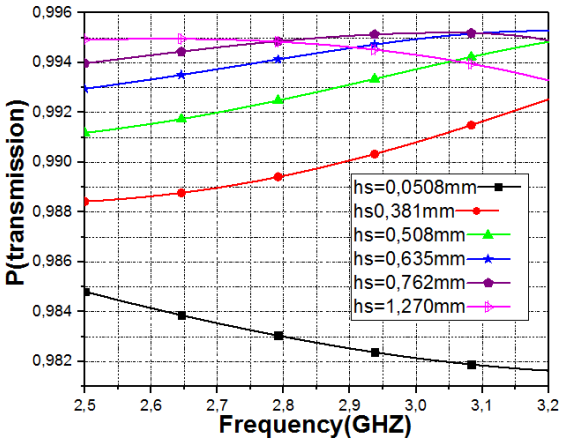

Figure2-25: transmitted power for different values of *hs*.

Through the simulation results, we notice that the optimum value of *hs* is (0.381mm) because they reflect power near to zero and the absorbed power equal to (0.008) and the transmitted power is 99%

Now all the parameters of the metamaterial unit cell are known, with the optimal thickness *hs* and the gap L_g and w , the structure metamaterial unit cell

In the next chapter we will use these optimal values of the metamaterial unit cell to design metamaterial real grid above a Microstrip patch antenna to enhance its performances such as gain bandwidth and the half power beam width HPBW…ete

2.9 Conclusion:

Homogenization theories are typically valid when the unit-cell size is much small compared to the wavelength. To extract the electromagnetic properties of metamaterials one method have been applied. The first one based on *S*-parameter which is suitable to be applied for both numerical simulation and experimental measurements in this chapter, we study a metamaterial and extract theirs electromagnetic parameters, this metamaterial can be used above a Microstrip patch antenna to enhance its performance.

3. Microstrip Antenna gain enhancement and widebandusing metamaterial for 5G application

3.1 Introduction

The metamaterials are considered the most important application in the field of antenna, which can improve its performance and reduce its size. The aim of this chapter is to enhance the antenna performance such as gain , bandwidth and half power beam width HPBWusing metamaterial lens, which is presented in chapter 2,

The metamaterial lens is placed on the top of a microstrip antenna at a distance *h* from the patch this distance can be optimized to obtain better antenna realized gain and wind bandwidth.

3.2 The proposed antenna design

In antenna engineering domain, researchers around the world have to resolve many fundamental challenges [36].Antennas have to conjugate at the same time a high gain, a wide bandwidth, a diversity of polarization and a reconfigurable , radiation pattern, while remaining the most compact possible. These characteristics are often conflicting, and the structured artificial materials bi- and three-dimensional such as metamaterials and/or electromagnetic/ photonic bandgap materials (E/PBG) can offer interesting solutions in this domain [36-37].

The design process of an antenna begins with understanding the application to be achieved and parameter requirements. Frequency is an important factor aids to determine the substrate to be used. After deciding the required data, the physical dimensions of the antenna are calculated. In this work using [38], we use Ansys High-Frequency Structure Simulator [HFSS v 13.0] to design and simulate two type of patch antenna at the operating frequency 28GHz for 5G application . The first antenna without slots is designed with the dimensions of Ls x Ws with a thickness d at the substrate. The substrate type of Rogers RT/Duroid 5880 with a relative permittivity of 2.2 and dielectric loss tangent of 0.0009. Further, the patch with dimensions Lp x Wp is mounted on the substrate, The probe feed consists of thedimensions Lf x Wf is represented in figure 3-1.

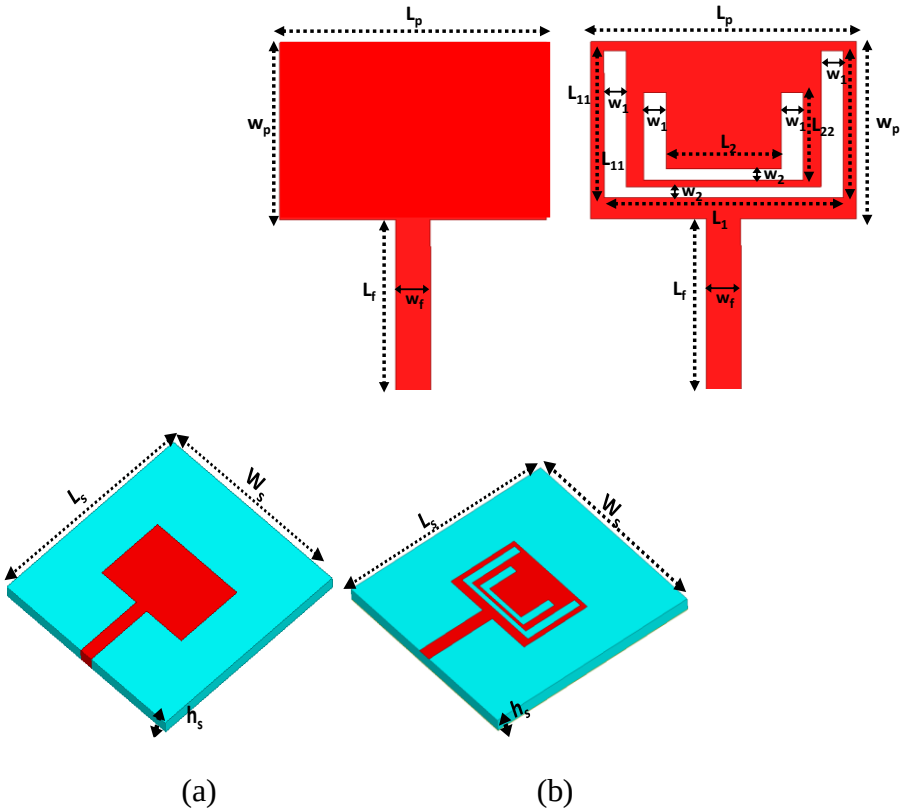

Figure 3-1: Patch antenna details :(a) patch without slots and (b) patch with slots.

The dimension of the patch antenna are show in table 3-1 ,The slots geometric parameters are adjusted to observe the variations concerning the gain, bandwidth, and resonant frequency of the proposed antenna.

Table3-1 Parametric dimensions of the designed antenna

parametres	Dimension (mm)	parametres	Dimension (mm)
Ls	12	L2	3.8
ws	12	L22	1.9375
d	0.508	wf	0.77
L11	3.2875	Lf	4
W1	0.15	Lp	3.1125
W2	0.15	wp	4
L1	5.4		

We compared the obtain results of a simple antenna (antenna without slots) to those of an antenna with slots, the antennas radiation patterns in E and H planes and the refraction coefficients are illustrated in figure 3-2 and 3-3. It is clear from the plot that loading a microstrip antenna with the slots enhances the antenna gain and the bandwidth at the operating frequency band 26-31 GHz.

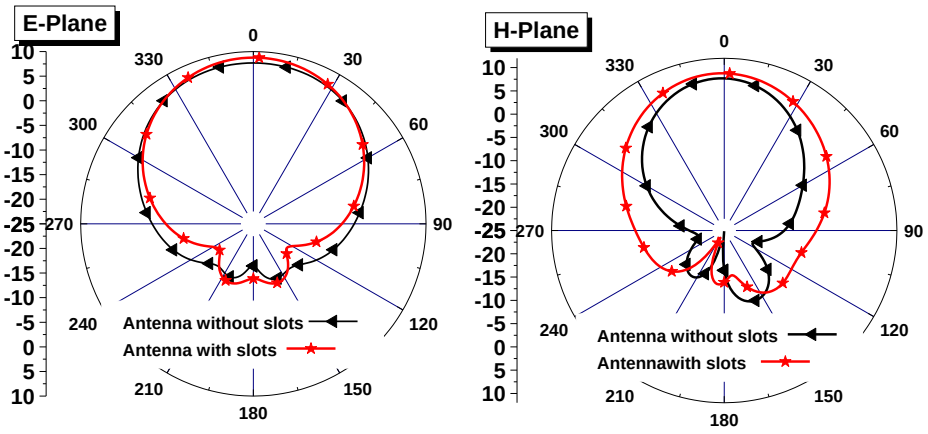

(a) (b)

Figure 3-2: Radiation pattern of the patch antenna with and without slots : (a) - E plane, (b) - H plane.

It is observed from figure 3-3 that the resonance of the proposed antenna is slightly shifted to lower frequency region, with good matching and wideband in the operating frequency band [27.4-30.7GHz].

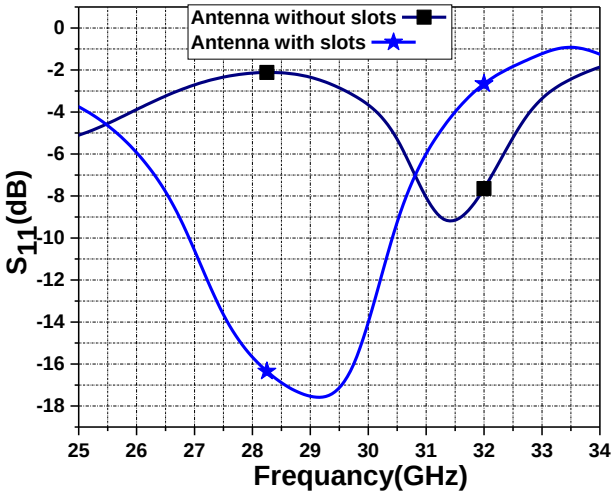

Figure 3-3: Reflection coefficient of the microstrip patch antenna with and without slots.

The antenna realized gain versus of the frequency is shown in figure 3-4 it can be seen that the antenna with slots provide gain enhancement in the operating frequency band 27.5Ghz -32GHz

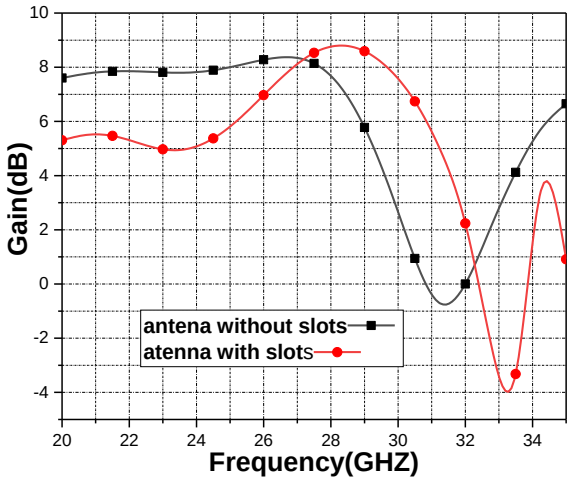

Figure 3-4: Realized gain of the microstrip patch antenna with and without slots:

The surface current distribution of the antenna with and without slots are presented in Figure 3-5 at the operating frequency 28 GHz. Larger amount of current flows below and above the U-slot in the microstrip patch, the antenna with slots provide good currents distribution.

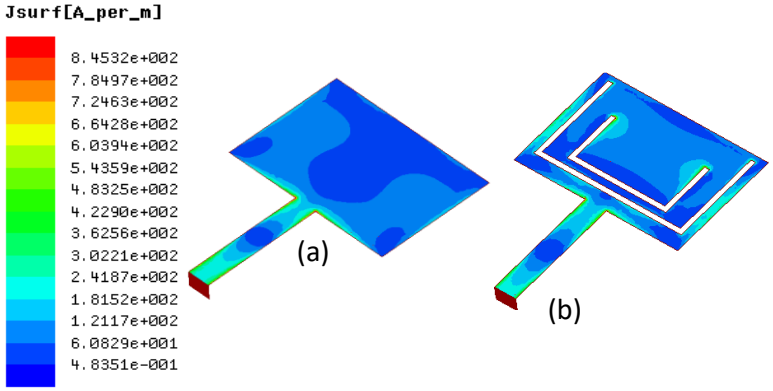

Figure3-5 : Simulated current distribution of antenna with and without slots

From Figure 3-6, shows the stable 3D far-field radiation pattern performance at three far frequencies in the operating band namely, at 26 GHz,28.5Ghz and 29.5 GHz, respectively

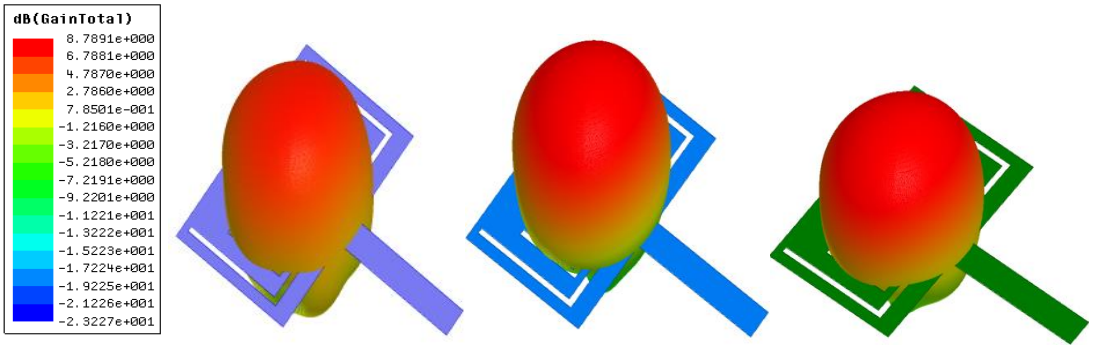

Figure3-6 :3D Radiation gain patterns calculated at ; (a) 26 GHz , (b) 28 GHz and (c) 29 GHz

The antenna realized gain of the proposed antenna is about 8.7dB if compared of the antenna without slots which is about 7.6dB, the proposed antenna enhance the antenna gain by about 1dB

In the next section we will use a metamaterial to enhance the antenna performance of this antenna.

We sommrized the obtaind results of the patch antenna with and wothout slots in table 2

Table 3-2 Half power beam width θ_{-3dB}(deg) and realized gain,bandwidth,s11 of the patch antenna with and without slots

	Realized gain(dB)	θ-3dB	φ-3dB	Bandwidth (%)	S11(dB)
Antenna without slots	8.3	89.2	54.86	-	-9.14
Antenna with slots	8.8	74.68	66.68	3.47	-17.58

3.3 Proposed antenna with metamaterial

The use of the metamaterial structures for enhancing antenna performances has been investigated by the number of authors [4, 5]. Among various unusual material properties, at microwave and millimeter-wave frequencies provided by metamaterials, permittivity/permeability and the refraction index.

The metamaterial as single layer superstreet suspended above a microstrip patch antenna (MPA), operating at 28 GHZ, for the gain enhancement and the bandwidth. The metamaterialsuperstrate layer is composed of a periodic arrangement of square SRR unit-cells, and behaves as an homogeneous medium . This metamaterial gathering radiatedwaves from the antenna and collimates them towards the superstreet normal direction. The proposed design improves the antenna gain by 4dB.

The unit-cells are arranged in an array with periodicity of 8 x 8, to design a layer of the metamaterial superstrate, as shown in figure 3-7 . The metamaterial superstrate covers the patch antenna and it functions like a lens being able indeed to improve the antenna performances such as gain, directivity, band width,…etc

The perspective view of the proposed antenna with metamaterial superstrate is shown in figure 3-8. The spacing from the radiator to the bottom of the metamaterialsuperstrate is h The

antenna ground plane and the metamaterialsuperstrate have dimensions of (L_S x W_S = (12 x 12) mm

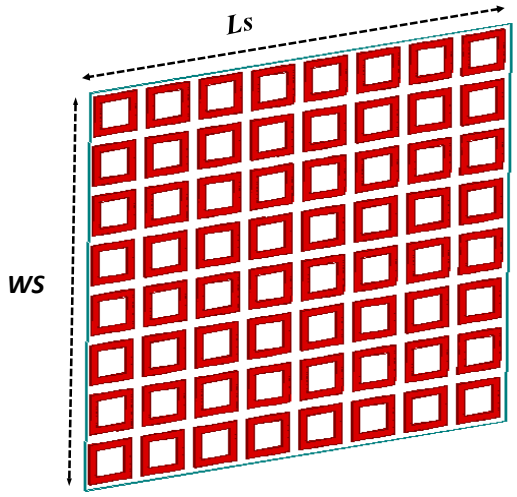

Figure 3-7 : Periodic structure of metamaterial

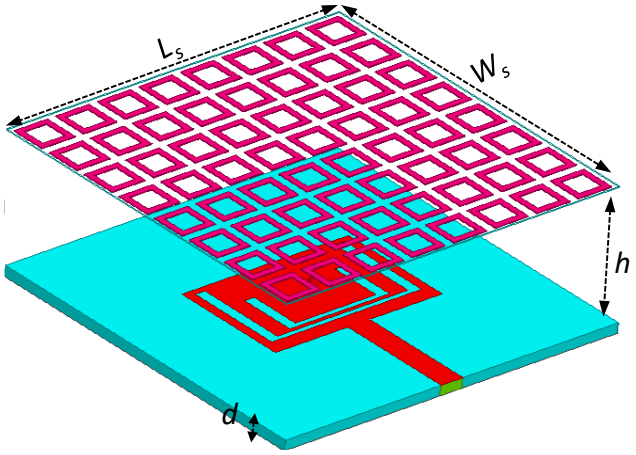

Figure3-8: The proposed antenna with metamaterials

The simulation results of the spacing parameter optimization h, for antenna metamaterial is presented in figure 3-9. From this figure, we observe that the spacing between the patch antenna and the superstrate layer is a key parameter in the antenna gain improvement. It can be optimized to obtain better antenna realized gain enhancement. A parametric study shows that the optimal value for the spacing is h = 7.2 mm as also shown in figure 3-9.

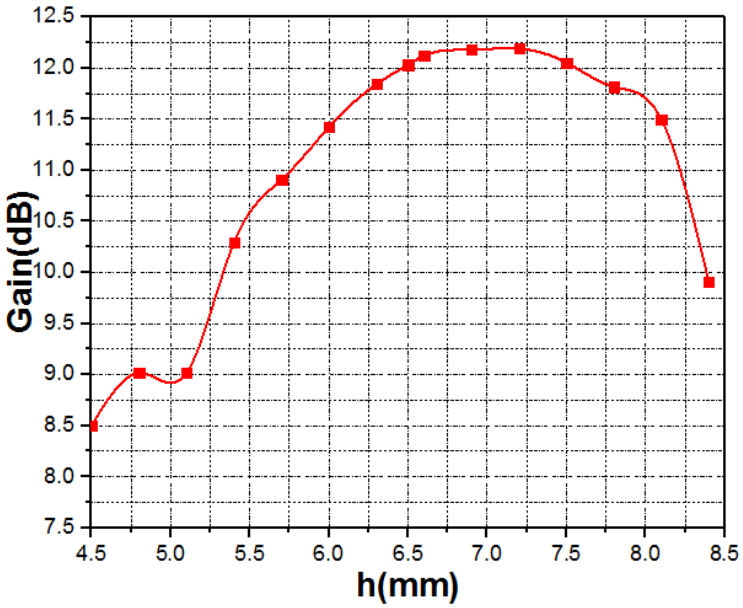

Figure 3-9 Realized gain of the proposed antenna with metamaterial for different spacing*h*.

And the spacing S between the metamaterial unit cell shown in figure 3-10 a key parameters that can be optimized to obtained better gain

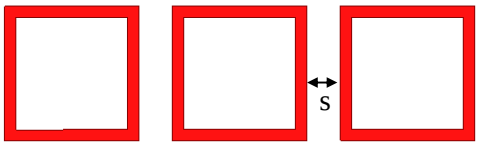

Figure 3-10 the spacingS between the elements metamaterial

It can be seen that from figure 3-11 the maximum realized gain of the optimal value of the spacing parameters S between the element is S=0.3mm correspondent a gain about 12.18 dB.

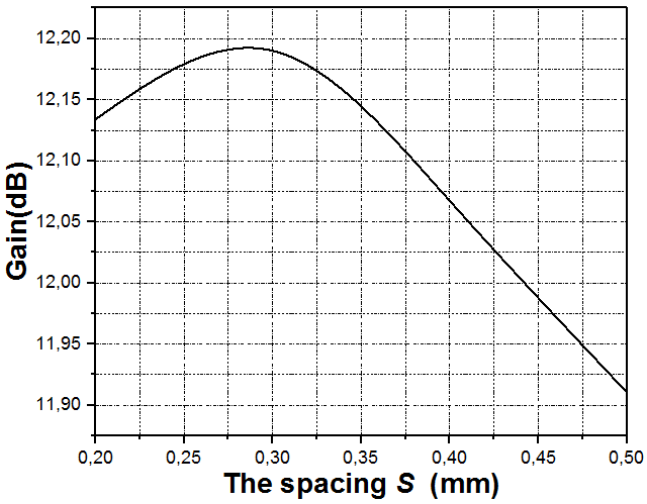

Figure 3-11 Realized gain of the proposed antenna with metamaterial for different spacing S.

A comparison between the antenna alone and the antenna with the metamaterial lenses

can be seen in figures 3-12 to 3-15. The radiation pattern, in the E and H plane, of the proposed antenna with and without metamaterial are shown in figures 3-11 and 3-12 .It is clear from the plots that the antenna is more directional with a metamaterial. The maximum realized gain obtained is 12.18 dB.The half-power beam width of the antennas, at the operating frequency, in E and H-plane respectively, are observed to be 74.68º and 66.68º, for the antenna alone, 35.21º and 36.24 º for the antenna with metamaterial superstrate which means a half-power beam width reduction of about 50%, in both E and H compared to the antenna alone

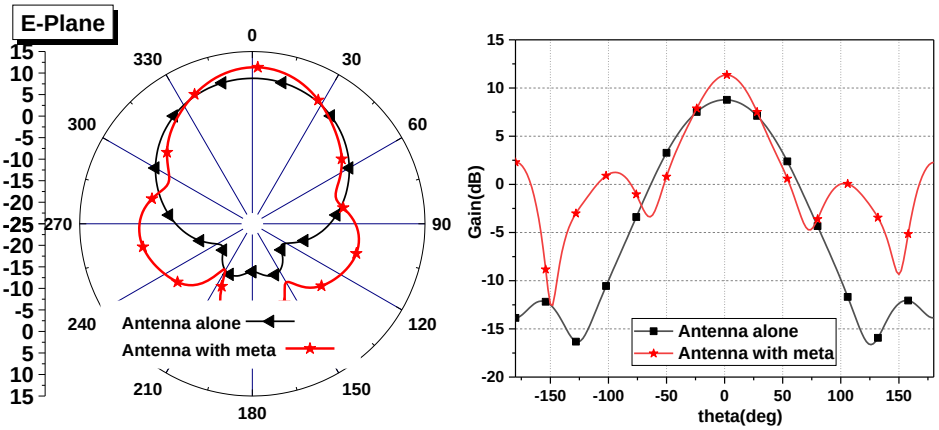

Figure: 3-12; Radiation pattern in E plane of the antenna with and without metamaterial.

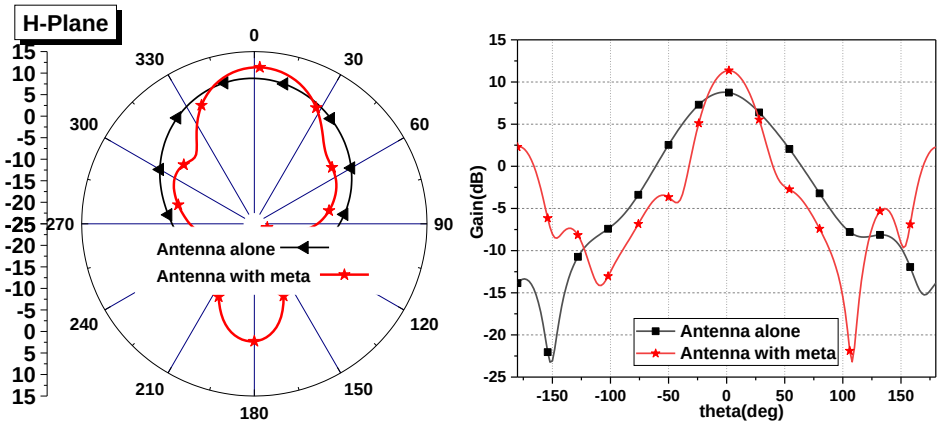

Figure: 3-13: Radiation pattern in H plane of the antenna with and without metamaterial.

The presence of the metamaterial, increases the antenna gain from 8.7 dB to 12.19 dB which corresponds to an enhancement the bandwidth from 3.2GHz to 5.2GHz 2.2GHz

Figures 3-13and 3-14 exhibits very promising results for an antenna with and without metamaterial at millimeter-wave frequencies. The return loss stays below -10dB from 27 GHz to 30.5 GHz for the antenna alone and from 25.2 GHz to 30.1 GHz for the antenna with metamaterial

The antenna realized gain versus frequency is shown in figure 3-14 it can be seen that the gain values ranges between 7.8dB and 7.5dB within the frequency band 27 GHz to 30.5 GHz for the antenna alone. The maximum gain of 8.7dB occurs close to 28.5GHz and the lowest S11 value of about -17.6 dB and the gain values ranges between 10.1dB and 10.05 dB within the frequency band 25.2 GHz to 30.1 GHz for the antenna metamaterial . The maximum gain of 12.19dB occurs close to 26 GHz and the lowest S11 value of about -17.6dB

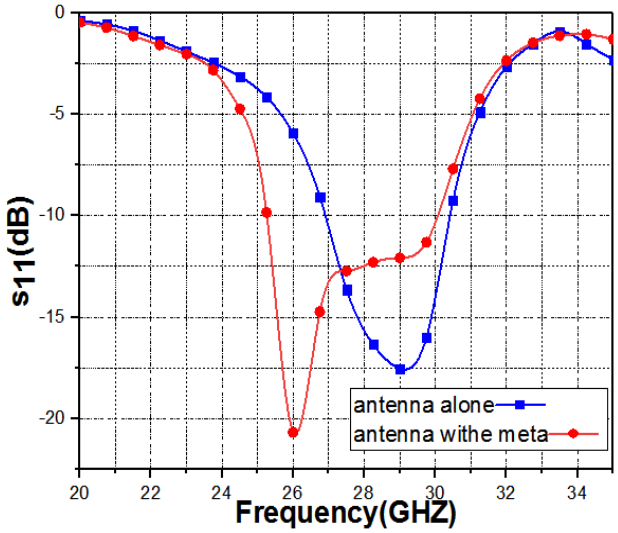

Figure 3-14 Return loss (S_{11}), for the patch antenna and the metamaterial patch antenna.

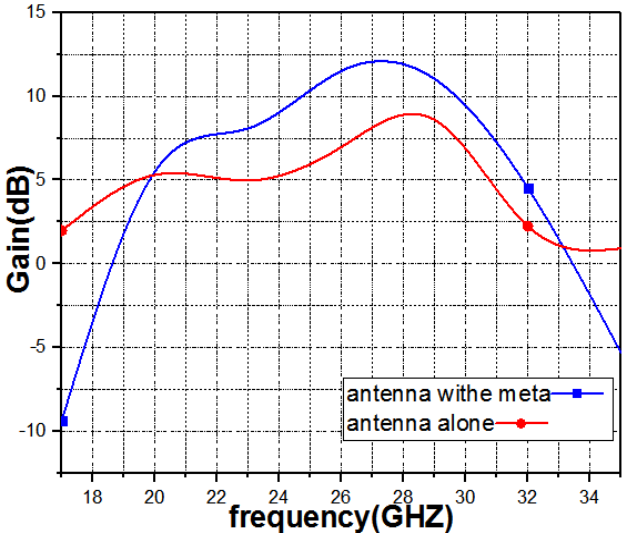

Figures 3-15 Calculated realized gain versus frequency

on the other hand, figurs 3-16 shows the stable far-field radiation pattern performance at three far frequencies in the operating band namely, at 26 GHz ,28 GHz and 29GHz, respectively. This further confirm the potential advantage of the proposed antenna with metamaterial .

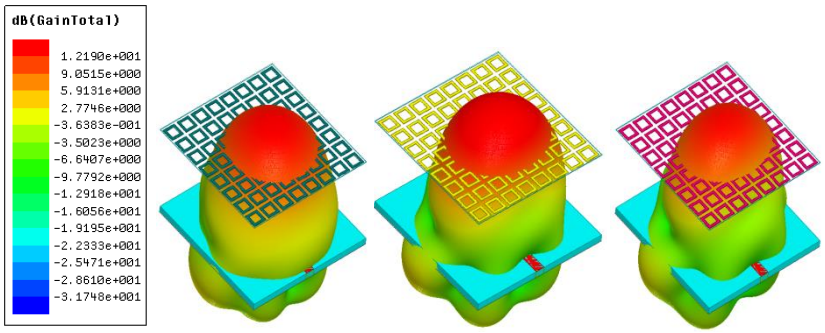

Figure3-16 :3D Radiation gain patterns calculated at ; (a) 26.5 GHz , (b) 28.5 GHz and (c) 29 GHz

We summarized the previous results in table 3-3 , from this table the metamaterial provide a gain enhancement and wideband at the operating frequency band 25.2GHz to 31 GHZ which corresponding of 5G application

Table 3-3 Half power beam width θ_{-3dB}(deg) and realized gain,bandwidth,s11 of the patch antenna with and without metamaterial

	Realized gain(dB)	θ-3dB	φ-3dB	Bandwidth(%)	S11(dB)
Antenna without slots	8.3	89.2	54.86	-	-9.14
Antenna with slots	8.8	74.68	66.68	3.47	-17.58
Antenna with metamaterial	12.19	35.21	36.24	5.21	-21.24

3.4 Conclusion

In this chapter we have proposed a micro strip antenna wideband and high gain for 5G application and we used the metamaterial to enhance the antenna performance:

i) The proposed antenna with slots, provided antenna realized gain about 8.7 dB and bandwidth about 3.2 Ghz

ii) The proposed antenna based of metamaterial provided gain about 12.19 and bandwidth about 5.2GHZ

Furthermore this structure enhances the antennas performances such as the gain and the bandwidth which makes is suitable for 5G systems

Conclusion

Our goal in thiswork isconsistto exploiting the potential offered by the metamaterials to design wideband antenna for 5G application. First we proposed antenna with dual U slots and we us the metamaterial to enhance the antenna performance, these metamaterials are artificial periodic structures which it is possible to tailor their constitutive parameters with any giving request. This metamaterial unit cell is used to design ametamaterial grid.This last are composed of an square ships with four slots,

Secondly,this metamaterial lens is obtained by a periodic structure based on metamaterial unit cell.

We characterized and optimized the elementary unit cell of the metamaterial unit cell by varying the dielectric thickness d, the width w, and the gap wg and Lg

The metamaterial was simulated with HFSS 3D simulator, and a first optimization was performed to obtain optimal reflection and transmission powers values

The optimized unit cell has a = 1.51mm, d = 0.381mm, w = 0.1 mm, εr = 9.4 and Lg = 0.1mm,wg=0 mm,t=0.035 mm

Once the metamaterials characterized and sized we have passed to the third stage of our work which are design and characterize the metamaterial lens (shape) Three types of metamaterial lens have beendesigned. Metamaterial layer superstrate placed above of the patch antenna.

Finally we started with the design of our patch antenna with dual U slots by HFSS software, and we used the metamaterial above the patch antenna to enhance the antenna performance wehave demonstrated the possibility of enhance the antenna gain and the bandwidth of the antenna.The antennarealized gain has enhancedwhere we obtained 12.19 dB with single metamaterial superstrate, and the bandwidth enhance by about 5.2GHz if compared with microstrip antenna which is 3.2 GHz

The half power beam width is reduced to 36° and 37° respectively in E and H plane for the antenna with metamaterial

References

[1]. Khan, Jalal, Daniyal Ali Sehrai, and Shakeel Ahmad. "Design and performance comparison of metamaterial based antenna for 4G/5G mobile devices." *International Journal of Electronics and Communication Engineering* 12.6 (2018): 382-387.

[2]. Bensafieddine, D., et al. "Agile radiation pattern control of metamaterial microstrip antenna." Applied Physics A 123.1 (2016): 1-6.

[3]. Chaker, S. M., and M. Bouzouad. "Metamaterial patch antenna radiation pattern agility." Applied Physics A 115.2 (2014): 459-465.

[4]. Dahlman, Erik, Stefan Parkvall, and Johan Skold. 5G NR: The next generation wireless access technology. Academic Press, 2020.

[5]. Alliance, N. G. M. N. "Recommendations for NGMN KPIs and Requirements for 5G." techreport, June (2016).

[6]. Mirfananda, Ahmad Salaam, and Muhammad Suryanegara. "5G spectrum candidates beyond 6 GHz: A simulation of Jakarta environment." 2016 IEEE Region 10 Symposium (TENSYMP). IEEE, 2016.

[7]. Asif, Saad. 5g mobile communications: Concepts and technologies. CRC Press, 2018.

[8]. Gangwar, Amit, and S. C. Gupta. "Metamaterials—A new era of artificial materials with extraordinary properties." International Journal of Engineering Research and Management Technology 1.2 (2014): 76-84.

[9]. Veselago, Victor, et al. "Negative refractive index materials." Journal of Computational and Theoretical Nanoscience 3.2 (2006): 189-218.

[10]. Schurig, David, et al. "Metamaterial electromagnetic cloak at microwave frequencies." Science 314.5801 (2006): 977-980.

[11]. Nouh, M., O. Aldraihem, and A. Baz. "Vibration characteristics of metamaterial beams with periodic local resonances." Journal of Vibration and Acoustics 136.6 (2014).

[12]. Mendhe, Shridhar E., and Yogeshwar Prasad Kosta. "Metamaterial properties and applications." International Journal of Information Technology and Knowledge Management 4.1 (2011): 85-89.

[13]. Engheta, N., and R. Ziolkowski, (eds.), "Metamaterials Physics and Engineering Explorations," New York: John Wiley & Sons, 2006

[14]. Wiltshire, M. C. K., ‘‘Bending of Light in the Wrong Way,’’ Science, 292, 2001, pp.60-61

[15]. Veselago, V. G., and E. E. Narimanov, "The Left Hand of Brightness: Past, Present andFuture of Negative Index Materials," Nature Materials 5, 2006, pp. 759-762

[16]. Sihvola, A., ‘‘Metamaterials in Electromagnetics,’’ Metamaterials, Vol. 1, Issue 1, 2007,pp. 2—11.

[17]. Cubukcu, Ertugrul, et al. "Split ring resonator sensors for infrared detection of single molecular monolayers." Applied Physics Letters 95.4 (2009): 043113.

[18]. Rennings, A., et al. "Double-Lorentz transmission line metamaterial and its application to tri-band devices." 2007 IEEE/MTT-S International Microwave Symposium. IEEE, 2007.

[19]. Eleftheriades, George V., and Keith G. Balmain. Negative-refraction metamaterials: fundamental principles and applications. John Wiley & Sons, 2005.

[20]. Abdulkarim, Yadgar I., et al. "Design and study of a metamaterial based sensor for the application of liquid chemicals detection." Journal of Materials Research and Technology 9.5 (2020): 10291-10304.

[21]. Chen, Tao, Suyan Li, and Hui Sun. "Metamaterials application in sensing." Sensors 12.3 (2012): 2742-2765.

[22]. Foner, Simon, and Brian B. Schwartz. Superconductor materials science: metallurgy, fabrication, and applications. Vol. 68. Springer Science & Business Media, 2012.

[23]. Fridman, Moti, et al. "Demonstration of temporal cloaking." Nature 481.7379 (2012)

[24]. Zhou, Hong, et al. "Terahertz biosensing based on bi-layer metamaterial absorbers toward ultra-high sensitivity and simple fabrication." Applied Physics Letters 115.14 (2019): 143507.

[25]. Anwar, RanaSadaf, Lingfeng Mao, and HuanshengNing. "Frequency selective surfaces: a review." Applied Sciences 8.9 (2018): 1689.

[26]. Kurra, Lalithendra, et al. "FSS properties of a uniplanar EBG and its application in directivity enhancement of a microstrip antenna." IEEE Antennas and Wireless Propagation Letters 15 (2016): 1606-1609.

[27]. Lubkowski, G., R. Schuhmann, and T. Weiland. "Extraction of effective metamaterial parameters by parameter fitting of dispersive models." Microwave and Optical Technology Letters 49.2 (2007): 285-288.

[28]. Davis, H. Ted. "The effective medium theory of diffusion in composite media." Journal of the American Ceramic Society 60.11.12 (1977): 499-501.

[29]. Gibson, Ronald F. Principles of composite material mechanics. CRC press, 2016.

[30]. Yoshida, Katsuhito, and Hideaki Morigami. "Thermal properties of diamond/copper composite material." Microelectronics reliability 44.2 (2004): 303-308.

[31]. Smith, David R., et al. "Direct calculation of permeability and permittivity for a left-handed metamaterial." Applied Physics Letters 77.14 (2000): 2246-2248.

[32]. Holloway, Christopher L., et al. "An overview of the theory and applications of metasurfaces: The two-dimensional equivalents of metamaterials." IEEE Antennas and Propagation Magazine 54.2 (2012): 10-35.

[33]. D.bensafieddine," Design of Metamaterial Agile Radiation Pattern Microstrip Antenna, these de magistaire" Universite Amar TelidjiLaghouat.Thesis 2015

[34]. S. M. Stanley et al., "A Dual-Band Dual-Polarised Stacked Patch Antenna for 28 GHz and 39 GHz 5G Millimetre-Wave Communication," *2019 13th European Conference on Antennas and Propagation (EuCAP)*, 2019, pp. 1-4

[35]. J. Saini and S. K. Agarwal, "Design a single band microstrip patch antenna at 60 GHz millimeter wave for 5G application," 2017 International Conference on Computer, Communications and Electronics (Comptelix), 2017, pp. 227-230.

[36]. Dubok, A., et al. "Fundamental challenges for wideband antenna elements in focal-plane arrays." 2015 9th European Conference on Antennas and Propagation (EuCAP). IEEE, 2015.

[37]. Ballestín-Fuertes, Javier, et al. "Role of wide bandgap materials in power electronics for smart grids applications." Electronics 10.6 (2021): 677.

[38]. Madhav, B. T. P., et al. "Measurement of dimensional characteristics of microstrip antenna based on mathematical formulation." Int. J. Appl. Eng. Res 9.9 (2014): 1063-1074.